SCIENCE CHINA
Technological Sciences

• Review •

September 2017 Vol.60 No.9: 1347–1364
doi: 10.1007/s11431-017-9058-8

Processing of advanced thermoelectric materials

LI JingFeng*, PAN Yu, WU ChaoFeng, SUN FuHua & WEI TianRan

State Key Laboratory of New Ceramics and Fine Processing, School of Materials Science and Engineering, Tsinghua University, Beijing 100084, China

Received March 19, 2017; accepted April 24, 2017; published online August 8, 2017

Last two decades have witnessed significant progress in thermoelectric research, to which materials processing has crucial contributions. Compared with traditional zone-melting method used for fabricating bismuth telluride alloys, new powder-based processes have more freedom for manipulating nanostructures and nanocomposites. Thermoelectric performance enhancement is realized in most thermoelectric materials by introducing fine-grained and nano-composite structures with accurately controlled compositions. This review gives a comprehensive summary on the processing aspects of thermoelectric materials with three focuses on the powder synthesis, advanced sintering process and the formation of nanostructures in bulk materials.

thermoelectrics, materials processing, nanostructured thermoelectric materials, mechanical alloying, spark plasma sintering

Citation: Li J F, Pan Y, Wu C F, et al. Processing of advanced thermoelectric materials. Sci China Tech Sci, 2017, 60: 1347–1364, doi: 10.1007/s11431-017-9058-8

1 Introduction

Thermoelectric materials that can be utilized for direct conversion between heat and electricity have drawn worldwide interests for decades [1]. So far, thermoelectric technology has been successfully applied in the field of electronic cooling, and a variety of thermoelectric coolers and temperature stabilizers are commercialized [2,3]. From the end of last century, unprecedented attention has been paid to thermoelectric research mainly because of increasing demands for the applications of energy harvesting from wasted heat sources by thermoelectric power generation. Great progress has also been achieved in the development of high-performance thermoelectric materials, which can be simply described by the rise of dimensionless figure of merit (ZT), defined as $ZT = (\alpha^2\sigma/\kappa)T$, where α, σ, κ and T are Seebeck coefficient, electrical resistivity, thermal conductivity, and absolute temperature, respectively [4]. Nowadays, high ZT > 2.0 have been reported for several materials even in the form of bulks, but ZT had remained below unity for almost three decades since 1960s [5–7]. High ZT values were obtained not only in some new compounds like skutterudites [8,9], half-Heuslers [10,11], clathrates [12,13] and selenides [14–18] but also in conventional Bi_2Te_3 [19–21] and PbTe [22–24] based materials. The progress should be attributed to the endeavors by the scientists from different fields including chemistry, physics and materials engineering. The advanced materials processing has more contribution to the ZT enhancement for conventional thermoelectric materials, which is especially important for widening the applications of thermoelectric technology. For example, so far Bi_2Te_3 alloys used in industries are fabricated by a conventional process based on zone melting and unidirectional solidification, by which high purity and crystallographic orientation can be controlled [25–27]. However, it is difficult to make a breakthrough to enhance the ZT of Bi_2Te_3 alloys fabricated

* Corresponding author (email: jingfeng@mail.tsinghua.edu.cn)

by the conventional process, whereas higher *ZT* values were achieved even in the same material system by introducing nanostructures via powder metallurgical (PM) process combining high energy balling and hot pressing or spark plasma sintering [19]. In addition, PM-processed Bi_2Te_3 alloys with refined grains have improved mechanical strength, which are suitable especially for manufacturing miniaturized modules [28,29].

It is clear that property enhancement benefits from processing development. So far, many new processes (maybe not new in other fields) have been applied to the synthesis of thermoelectric materials, so it should be timely for us to review the progress achieved for thermoelectric materials processing. There are many excellent review articles [4,7,30–36] summarizing the current status of thermoelectric research, but most of them are based on the viewpoint of materials science, in which the importance of materials processing has not been emphasized. In this review, we want to give a comprehensive summary of materials processes by stressing their contribution to the property enhancement. It is our great pleasure if this work could provide certain reference and shed light on the development of thermoelectric materials with higher performance in the future.

2 Synthesizing process of thermoelectric compounds

The synthesis process is the key step to obtain interested thermoelectric compounds. The past two decades have witnessed a bloom of various methods for synthesizing a diversity of thermoelectric materials. The traditional techniques, melting and solid-state reaction, are still well used and keep producing high-performance materials. Meanwhile, high-energy ball milling including so-called mechanical alloying (MA) has been widely employed for synthesizing fine powders of thermoelectric compounds [30]. In addition, recent studies revealed that many thermoelectric compounds can be easily synthesized by self-propagation high-temperature synthesis (SHS) [37]. Certainly, chemical synthesis routines, such as hydrothermal and/or solvothermal methods are powerful in making fine powders with controllable morphology and dimensions/sizes. Thermoelectric materials in the bulk form are usually fabricated by combining two methods; one for synthesizing powders and one for sintering. Sometimes to reduce the grain sizes, ingots fabricated by the melting and casting method are intentionally pulverized and then sintered again. For example, layered compounds prepared by melting or zone-melting tend to have very large grains and are subjected to severe cleavage problems. In this regard, powder-processing and sintering techniques are introduced to strengthen the samples and further purify the phases, which will be discussed in Section 2.2 and 3, respectively.

In this section we summarize several typical methods that are frequently used in synthesizing thermoelectric materials. Particularly, we shall put an emphasis on the newly emerging techniques on polycrystalline materials, describing their working principles and trying to establish a link among the method, microstructure and the consequent thermoelectric properties. Figure 1 shows the yearly publications from 2000 to 2016 about thermoelectric materials fabricated by different methods.

2.1 Melting

Melting technique has long been a conventional method for producing thermoelectric materials. For example, zone-melting, a unidirectional solidification process has been employed to manufacture Bi_2Te_3 in industry, which can produce cylindrical ingots with a diameter of 17 mm or even 25 mm [38]. While in laboratory, researchers prefer the glass-encapsulated melting methods to produce thermoelectric alloy ingots on a small scale, with several pre-treatments including cleaning and heat treating of the quartz tube, coating the wall with carbon when reactive elements are involved, and baking to ensure all organic residues being burned. In some particular materials systems, some post-treatments like optimizing the cooling rate of as-melted ingots are also significant in order to control the size and morphologies of nanostructures in host materials [39,40].

Melting techniques can be differentiated by their heating resources (including voltaic arc, eddy current or electric resistance), atmospheres (air, protective gas or vacuum), or circumstances (e.g., under a magnetic field or not). Especially for thermoelectric research, some widely-spread methods, including arc-melting, induction melting and levitation melting, are intentionally selected in accord with the peculiarities of starting reactants and resultant compounds.

In general, the melting processing, in which the reactants are heated above the highest melting point of them or the resultant compounds, is often proceeded in an ordinary box furnace with electric resistance heating, e.g., a muffle. For most of the state-of-the-art thermoelectric compounds without high melting temperatures (lower than 1800°C), they are often produced by such methods, such as bismuth tellurides ($Bi_2Se_xTe_{3-x}$, $Bi_{2-x}Sb_xTe_3$) [41], lead chalcogenides (PbTe

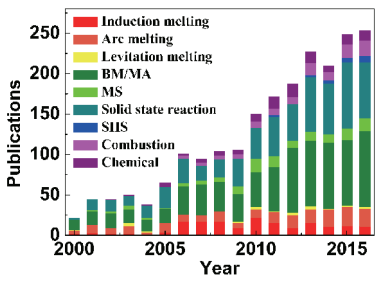

Figure 1 (Color online) Yearly publications related to thermoelectric materials processed by different methods.

[42–44], PbSe [45], PbS [46]), copper chalcogenides ($Cu_{2-x}Se$ [47], $Cu_{2-x}S$ [48]), tin chalcogenides (SnSe [49,50], SnTe [51]), metal silicides (Mg_2Si [52], $MnSi_{1.7}$ [53]) and Cu-Sb-Se/S ternary compounds (Cu_3SbSe_4 [54], $Cu_{12}Sb_4S_{13}$-based tetrahedrites [55]), etc. However, for some transitional metals with extremely high melting points, it becomes more difficult to melt all the reactants in these box-type furnaces, therefore arc melting or induction melting is often used.

Induction melting is a widely used melting technique in industry. For this technique, an electrically conducting object (usually a metal) is heated by electromagnetic induction, where heat is generated in the object by eddy currents because of the rapidly alternating magnetic field that comes from a high-frequency alternating current (AC) through the electromagnet [56]. The eddy currents flow through the resistance of the material and thus heat it by Joule heating. Induction heating is used in many industrial processes, such as heat treatment in metallurgy, Czochralski crystal growth, zone refining in semiconductors and melt refractory metals that require very high temperatures. For thermoelectric research, a variety of materials with metallic reactants, such as skutterudites [57], half-Heuslers [58] and clathrates [13], have been produced through the induction-melting method.

The arc-melting method is based on electric arc. In a typical arc-melting process, the arc forms between the charged material and the electrode, and then the former is heated by both the current passing through and the radiant energy generated by the arc [59]. The arc temperature can reach 3000°C, which enables the melting of even the most reactive and refractory metals, usually in vacuum or inert-gas atmospheres. One benefit of this method is its great flexibility as the processing can be readily and rapidly started or stopped. Besides, both reactive metals like titanium and refractory ones like tungsten can be arc-melted, which provides more alternatives in designing thermoelectric alloys, Cu- and Ni-substituted clathrates [13], Sn-alloyed half-Heuslers [60] and B- or P-doped $Si_{1-x}Ge_x$ alloys [61]. Moreover, another drawback of conventional melting methods is the inhomogeneity of the products especially for some alloys like half-Heusler (HH) compounds, due to static melting without mechanical stirring. Instead, levitation melting, where a magnetic field (usually using an extra coil) is coupled with the primary induction heating mode, is successful to fabricate such metallic alloys [11,62,63]. It is usually proceeded in a high-frequency furnace, where the heat is generated inside the object itself rather than by an external heat source via conduction. Therefore, no external contact is needed, which is important when contamination is an issue.

2.2 Powder-based processing

2.2.1 Ball milling

Ball milling (BM) is a simple process, which has attracted increasing interests for years in the field of thermoelectrics as one of the most effective powder processing technique. BM includes mechanical grinding (MG) and mechanical alloying (MA). In addition to the grinding effect, the MA process can lead to the compound synthesis from elemental powders by the mechanochemical effect [64,65]. Usually, MA is conducted in a dry milling form, so that the collision energy between balls can be effectively transferred to milled powders. There are multiple types of BM machines, among which planetary, shaker and mixer mills are commonly used. Nevertheless, the operating principles are almost the same. The inertia of the grinding balls give high-energy impact on the particles, which involves cold welding, fracturing, and re-welding, leading to further pulverization [64]. Featured with cost effectiveness and high efficiency, BM is widely used in materials research. Moreover, the three main applications, i.e., producing fine grained or nanostructured powders [19,66], synthesizing compounds [67–72] and mixing composites [73,74] make BM particularly popular in thermoelectric community. The intensity of BM can be tuned by adjusting the amounts of balls, ball milling speed and time, as well as the ratio of the big balls to small ones. Additionally, organic agent like stearic acid is sometimes used to facilitate the pulverization process and prevent excessive cold welding especially when ductile powders are milled [64], and ethanol can benefit the collection of the refined powders. The process of BM is schematically illustrated in Figure 2.

As aforementioned, due to the high energy of mechanical effects, BM is effective to obtain fine or even nano-sized powders. The refined structures would greatly strengthen the scattering of phonons and thus significantly reduce the thermal conductivity if they could be retained after solidification. In 2008, Poudel et al. [19] reported that excellent performance of p-type nanocrystalline BiSbTe bulks with a peak *ZT* of 1.4 could be achieved by simply ball milling the commercial ingots combined with subsequent hot pressing (HP). The greatly enhanced thermoelectric performance mainly benefits from the significant reduction of thermal conductivity. Nanograins and nanodots induced by BM and HP are considered to be responsible for the large decrease of thermal

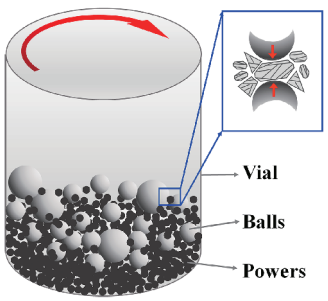

Figure 2 (Color online) Schematically illustration of BM. Coarse powders or chunks are pulverized and mixed during BM. Fine and homogenous powders are obtained.

conductivity by acting as the phonon scattering centers. In addition, the bipolar effect is also suppressed after BM and HP, probably due to the nanostructure-induced interfacial potential that scatters more minority carriers. Such *ZT* enhancement by introducing nanostructures through BM and HP has also been achieved in half-Heuslers [60,75], p- [76] and n-type [77] SiGe by the same group. In recent years, not only 3-D nanocrystalline [19], but also other nanoscopic structures like 1-D point defects [21,29] and 2-D dislocations [20,21] are widely employed to decrease the thermal conductivity. By BM one can construct such a hierarchical structure composed of 1-D point defects, 2-D dislocations and 3-D nanograins that can effectively scatter phonons over the broad wavelength spectrum and thus reduce the thermal conductivity [78]. Besides pulverizing and introducing *in situ* nanostructures, BM is also very effective for creating homogenous nanocomposites. In 2013, Li et al. [73] achieved a high *ZT* for BiSbTe nanocomposites by embedding small amounts of SiC nanoparticles via MA and SPS. Since MA is a mechanochemical process, by which BiSbTe grains were presumed to form on the surfaces of SiC nanoparticles, resulting in well bonded interfaces between SiC dispersion and BiSbTe matrix. As a result, it is possible to simultaneously enhance the Seebeck coefficient and electrical conductivity in this composite material, in addition to the effect of reducing lattice thermal conductivity.

On the other hand, it is worth noting that besides the effectiveness for reducing thermal conductivity, BM also shows significant influence on the electrical transport properties. This is not only because that the carriers transport is impeded by scattering from nanostructures, but also the variation of charge carrier concentration induced by BM. The carrier concentration is affected when charged point defects are introduced during BM, which is particularly obvious in Bi_2Te_3-based alloys [41,67]. As is known, a zone melting Bi_2Te_3 ingot is always p-type due to the formation of negatively charged antisite defects [79]; however, it changes to n-type when subjected to BM because of the large amounts of anion vacancies [79] and donor-like effect [80]. Pan et al. [29] has compared thermoelectric properties of the ingots and the spark plasma sintered bulks (BM+SPS samples) using the powders directly pulverized from the corresponding ingots for both p- and n-type Bi_2Te_3 based alloys. It is found that the in the BM+SPS samples the hole concentration of p-type BiSbTe alloys decreases while the electron concentration of n-type BiTeSe materials are increased. The reasons are ascribed to the formation of positively charged anion vacancies as well as the donor-like effect that are induced by strong mechanical deformation. A considerable variation in carrier concentration would consequently affect the electrical conductivity and the Seebeck coefficient in a reverse direction accordingly. Therefore, how to gain a high thermoelectric performance with an optimal carrier concentration by carefully tuning the charged point defects are raising more and more attention. Hu et al. [41] enhanced the thermoelectric properties of both p-type BiSbTe and n-type BiTeSe alloys by atomic scale point defect engineering. Pan et al. [67] also studied thermoelectric properties of n-type BiTeSe (prepared by MA and SPS) from the view of charged point defects. It should also be noted that the transport properties of p-type BiSbTe is less influenced by the charged point defects than the n-type counterpart. As pointed by Liu et al. [81], the free carrier concentration of n-type BiTeSe is five times more scattered than p-type BiSbTe with the same concentration of Te evaporation. This is also the reason why the n-type BiTeSe has a much poorer reproducibility under BM process. BM-induced variation in carrier concentration has been found in many other thermoelectric materials as well, such as the newly emerging BiCuSeO [82] and SnSe [83], which is also probably related to the formation of certain point defects.

As a simple and cost-effective method, BM has been applied to almost all classes of thermoelectric materials (Table 1) [71,72,84–92]. In 2014, Tan et al. [93] first reported an earth-abundant and environmentally friendly SnS thermoelectric material fabricated by MA and SPS with a promising *ZT* of 0.6 (Ag doped). Wei et al. [94] fabricated high quality Sn-doped Cu_3SbSe_4 samples by MA and SPS and found a nearly ideal doping efficiency and well modeled transport properties. Particularly, BM is capable of synthesizing a variety of materials that can be hardly fabricated by liquid methods. Traditional melting synthesis requires high temperatures and certain atmosphere, which are not only time consuming but also would probably result in inhomogeneous samples as vapor phase loss of elements or oxidation may occur at elevated temperatures. Moreover, the occurrence of eutectic and peritectoid reactions in some materials systems are also hard to avoid during melting. In contrast, MA can synthesize composites at room temperature in a short time, which largely reduces the cost and is environmentally friendly. And since MA is a completely solid-state processing technique, the materials that are hard to obtain by melting method like $La_{3-x}Te_4$ [95] and FeSi [96] thermoelectric materials could be successfully synthesized by MA. Nevertheless, MA also has its own limits in fabricating some materials in which impurity phases may be very difficult to be removed. For example, Wei et al. [97] reported that small amounts of Cu_3SbSe_4 always appeared when synthesizing Cu_3SbSe_3, even after annealing. Zou et al. showed that single phase could hardly be obtained via MA for either TiNiSn [98] or FeVSb [99] half-Heusler alloys. Fortunately, these thermoelectric materials can be successfully synthesized by the melting methods.

At last, BM can also be utilized to enhance the mechanical properties of materials, especially for layer structured compounds like Bi_2Te_3 with cleavage nature. Pan et al. [29]

Table 1 Representative works based on BM

Type	Material	Method, *ZT*@*T*(K)	Reference
Bi_2Te_3 based alloys	BiSbTe	Ingots-BM+HP, 1.4@373 K	[19]
	BiSbTe@SiC	MA+SPS, 1.33@373 K	[73]
	BiSbTe	Melt-BM+HP, 1.3@380 K	[41]
	n-type Bi_2Te_3	Melt-BM+HP, 0.72@373 K	[100]
	BiTeSe	MA+SPS, 0.82@473 K	[67]
PbTe based alloys	PbTe@Tl	BM+HP, 1.3@673 K	[69]
	PbSe@Al	BM+HP, 1.3@850 K	[101]
	$Ag_{0.8}Pb_{18+x}SbTe_{20}$	MA+SPS, 1.37@673 K	[91]
	$AgPb_mSbTe_{m+2}$	Repeated MA+SPS, 1.54@723 K	[102]
	$AgSn_mSbTe_{m+2}$	MA+SPS, 0.8@723 K	[103]
	$Pb_{1-x}Sn_xSe$	MA+SPS, 1.0@773 K	[68]
Skutterudites	$CoSb_{3-x}Te_x$	MA+SPS, 0.93@820 K	[104]
	$CoSb_3$	BM, none	[92]
	$CoSb_{3-x}Te_x$	MA+SPS, 1.1@823 K	[105]
	Cu_3SbSe_3	MA+SPS, 0.25@650 K	[97]
	Cu_3SbSe_4	MA+SPS, 0.7@673 K	[94]
Selenides and sulfides	$CuFeS_2$	MA+SPS, 0.21@573 K	[88]
	$Cu_{1.96}S$	MA+SPS, 0.5@673 K	[86]
	SnS	MA+SPS, 0.16@823 K	[106]
	SnS@Ag	MA+SPS, 0.6@873 K	[93]
Half-Heuslers	(ZrHf)Co(SbSn)	Ingot-BM+HP, 0.8@973 K	[60]
	FeVSb	MA+SPS, 0.31@573 K	[99]
	TiNiSn	MA+SPS, 0.32@785 K	[98]
	(HfZr)Ni(SnSb)	Melt-BM+HP, 1.0@873 K	[75]
HMS	HMS	BM+SPS, 0.39@770 K	[85]
	$MnSi_{1.75-d}$	MA+HP, 0.28@823 K	[90]
	$MnSi_{1.73}$	BM+PDS, 0.47@873 K	[87]
	$La_{3-x}Te_4$	MA+HP, 1.1@1275 K	[95]
Others	BiCuSeO	Solid state reaction+BM+SPS	[82]
	BiCuChO	MA+SPS, none	[107]
	$Mg_2Sn_{0.75}Ge_{0.25}$	BM+HP, 1.4@723 K	[89]
	p-type SiGe	BM+HP, 0.95@1173 K	[76]
	n-type SiGe	BM+HP, 1.3@1173 K	[77]

compared the mechanical strength of Bi_2Te_3-based ingots and MA+SPS polycrystalline, and demonstrated that the MSP (modified small punch load) strength improved more than three times and the hardness enhancement is over 60% after MA and SPS. The reasons for the large enhancement of mechanical strength by MA and SPS could be attributed to grain refinement and mixed orientations of cleavage plans. The enhanced mechanical strength would be advantageous for practical manufacturing and devices' application.

2.2.2 *Melt spinning*

Melt spinning (MS) is an efficient method for rapid cooling of molten liquids. The working principle of MS is depicted in Figure 3(a). A thin stream of molten alloy is injected onto a wheel (roll, drum etc.) that is rotated and internally cooled. The heat of the melts is rapidly transferred to the wheel, which incurs a fast solidification and even amorphization of the liquid, continuously producing thin tapes or ribbons as seen in Figure 3(b) [108–110]. The cooling rate can be as high as 10^4–10^7 K min^{-1} [111], so greatly retained nanostructures, notably refined grain sizes and even amorphous phases can be obtained [112]. The microstructure of the ribbons depends strongly on the local temperature and cooling rate as seen in Figure 3(c) and (d) [109], and can be readily controlled by adjusting the processing parameters in MS [113]. Simply speaking, by increasing the wheel speed, the cooling rate is monotonically enhanced and the ribbons get thinner. With a larger ejection pressure, both the cooling rate and ribbons'

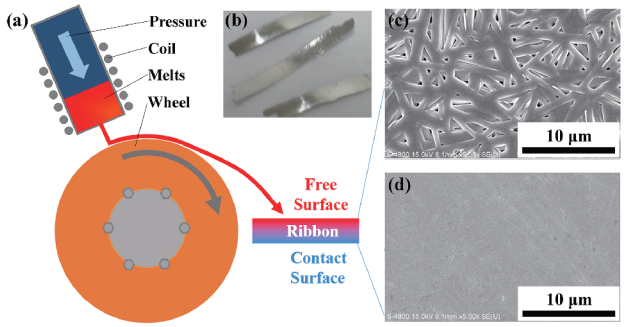

Figure 3 (Color online) (a) Schematic diagram of a melt-spinning apparatus; (b) photo of melt-spun BiSbTe ribbons, SEM morphologies of the (c) free and (d) contact surface. (b)–(d) reprinted from ref. [109], with the permission of AIP Publishing.

thickness are found to increase [114].

The history of MS can be dated back to late 1950s when Pond was granted a series of patents on this technique, and outlined the current concept with Maddin [115–117]. Preliminary application of MS in fabricating thermoelectric materials was initially reported in 1990 by Dey [118] on BiSb alloys that exhibited a maximum ZT = 0.14 at room temperature. In the early years of this century, Lee et al. [119] reported a ZT = 2 in melt-spun amorphous Si-Ge-Au compounds, but this work did not raise widespread attention. Very soon after that, Kim et al. [120], Chen et al. [121] and Zhao et al. [122] prepared BiSbTe and $FeSi_2$ thermoelectric alloys using MS and obtained satisfactory performance. However, this technique had still not received great attention in thermoelectric community until 2007 when Tang et al. [108] successfully spun BiSbTe compounds with a high ZT = 1.35 and demonstrated the unique nanostructures introduced by this method. Since then, Tang's group and others carried out a series of studies on a large variety of thermoelectric materials by using MS. High ZT values have been obtained in Bi_2Te_3-based compounds, skutterudites, silicides, $(GeTe)_x(AgSbTe_2)_{1-x}$ (TAGS), Zn_4Sb_3 and half-Heusler alloys, etc. Representative studies from 2000 to 2015 are summarized in Table 2.

Special micro- and nano-structures are usually present in these MS-processed samples and found to largely contribute to high thermoelectric performance, which are of great interest to the research community. For examples, in p-type $Bi_{0.52}Sb_{1.48}Te_3$ bulk materials prepared by MS combined with SPS [109], unique low-dimensional structures were observed, consisting of an amorphous structure and 5–15 nm nanocrystalline regions with coherent interfaces. The amorphous and nano-featured structures are believed to strongly scatter phonons while the coherent interfaces can provide a path for charge conduction, which is beneficial to the overall enhancement of thermoelectric performance. In addition, by virtue of this technique hierarchical structures and *in situ* nanoscale precipitates are also found in BiSbTe compounds, leading to a simultaneous enhancement in not only thermoelectric performance but also mechanical strength and thermal stability [28].

2.2.3 *Self-propagating high-temperature synthesis*

The self-propagating high-temperature synthesis (SHS) is an autowave process analogous to the propagation of a combustion wave, in which the synthesis is initiated by point heating a small part of the sample [37,131], as illustrated in Figure 4. In this process, a chemical reaction is localized in the combustion zone that spontaneously propagates over a chemically active medium. As the combustion wave passes through the sample it purifies the materials and maintains its stoichiometry [132]. This technology is actively exploited in inorganic materials, being effective to produce powders, compact materials and workpieces as well as make coatings and weld component parts.

The appealing attributes of the SHS synthesis, namely its fast one-step process requiring minimum of energy, scalable nature, and maintaining of the stoichiometry, make it popular in synthesizing a wide range of thermoelectric materials, including Cu_2Se [37], Bi_2Te_3 [133], SnTe [134], Mg_2Si [135,136], skutterudites [137], half-Heusler alloys [37],

Table 2 Selected studies on melt-spun thermoelectric materials

Type	Material	Method, ZT@T(K)	Reference
Bi_2Te_3-based alloys	$Bi_xSb_{2-x}Te_3$ x unspecified	ZM-MS-SPS, 1.35@ 300 K	[108]
	$Bi_{0.52}Sb_{1.48}Te_3$	ZM-MS-SPS, 1.56@ 300 K	[109]
	$Bi_2(Te_{0.8}Se_{0.2})_3$	MS-SPS, 1.05@420 K	[123]
	$Bi_{0.5}Sb_{1.5}Te_3$	ZM-MS-PAS, 1.22@340 K	[28]
Skutterudites	$Yb_{0.2}Co_4Sb_{12.3}$	MS-SPS, 1.26@ 800 K	[124]
	$CaFe_3CoSb_{12}$	MS-SPS, 0.9@773 K	[125]
Silicides	$Fe_{0.92}Mn_{0.08}Si_2$	LM-MS-HP, 0.17@ 973 K	[121]
	$MnSi_{1.75}$	IM-MS-SPS, 0.65@ 850 K	[126]
	$Mg_2Si_{0.3}Sn_{0.7}$	MS-PAS, 1.3@750 K	[127]
Others	$Hf_{0.6}Zr_{0.4}NiSn_{0.98}Sb_{0.02}$	LM-MS-SPS, 0.9@ 900 K	[128]
	$(Zn_{0.99}Cd_{0.01})_4Sb_3$	MS-SPS, 1.30@700 K	[129]
	TAGS-85	MS-HP, 1.6@750 K	[130]

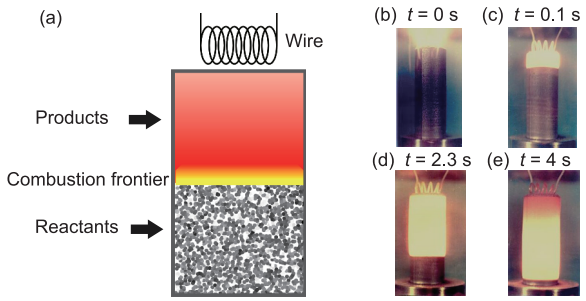

Figure 4 (Color online) Schematic drawing of SHS process (a) and photos of reactions at the shown times (b)–(e). (b)–(d) are taken from ref. [131], © 2011 Erausquin JI. Published in [Processing and Specific Applications, InTech, 2011], under CC BY-NC-SA 3.0 license. Available from: http://dx.doi.org/10.5772/17044.

BiCuSeO [138] and other oxides [139,140]. In the case of a solid SHS process between two reactants, the combustion reaction proceeds in a diffusion mode, where the reaction rate is limited by the diffusion of the second component through the product layer. Owing to the high diffusion resistance of contacting areas of the particles, recrystallization processes are virtually completely suppressed in such systems.

As a result, nanoscopic products are easily obtained from the nanosized reactants. Together with the ability of maintaining desired stoichiometry, SHS technique provides an alternative way for introducing *in situ* nanostructures in the resultant reactants. For example, Su et al. [37] successfully synthesized thermoelectric Cu_2Se compounds by such SHS techniques, in which the product's composition was precisely controlled ($Cu_{2.004}Se$ in products from nominal Cu_2Se composition). In addition, typical corn-like distributed nanodots of 5–10 nm were prevailingly formed throughout the matrix of micron-scale size, where their interfaces are basically coherent, greatly enhancing phonon boundary scattering while remaining excellent electrical properties. Similarly, Li et al. [141] prepared (Ag, In)-co-doping Cu_2SnSe_3 via a fast and one-step combustion synthesis, where secondary SnSe phase was observed separately distributed in the matrix. The dispersion of these SnSe precipitates creates lots of interfaces between them and the matrix, which was believed to be helpful for the phonon scattering leading to the reduction of thermal conductivity.

The SHS of nanosized materials is most influenced by mechanical treatment of products [132]. Firstly, mechanical activation of reactants before initiation is of great significance as it increases the reactivity of reactants by increasing defect concentration and/or the reaction area (due to a decrease in the particle size). Secondly, the mechanical activation can influence the rate and conditions of the combustion front propagation (macro-kinetic effect) as well as the shape and size of the crystallites and porosity of the structure (structural effect). However, a precise control on processes of the wave propagation and the structure formation is a challenging task. Thirdly, grinding of combustion products, for instance, mixing and ball milling, are also efficient ways to produce nanosized particles.

2.2.4 Soft chemical reaction

Soft chemical reaction methods, or called as wet process, are increasingly employed for the processing of thermoelectric materials despite its complexity as compared with the physical methods mentioned above [142]. In particular, nanostructures of thermoelectric compounds with controlled morphology can be synthesized by the wet processes with the advantages of low synthesis temperature and fine grain sizes in comparison with those by a high temperature route such as melting process [143]. By now, the most widely used soft chemical methods include hydrothermal/solvothermal method, sol-gel technique and microwave-assisted solution synthesis. This section highlights recent progress of the solution-based synthesis and discusses the advantages and disadvantages.

Hydrothermal method has been used as an effective technique for synthesizing size- and shape-controlled nanostructured materials and attracted more and more attention over the past few decades [144,145]. For this technique, precursor materials (usually metal salt or metal oxide) combined with special templates in stoichiometry are dissolved in aqueous solution system, which is then loaded, sealed, heated into an autoclave to a desired temperature for a period of time and then cooled to room temperature. The interior reaction conditions were strictly controlled, such as templates/additives concentration, pH value and pressure. It is noted that the grain size and morphology can be largely modified by exterior conditions, including the reaction temperature and time and sonication/stir mixture treatment time. A major benefit of hydrothermal method lies in the controllable doping of foreign ions and optimizing the nanostructures of grain orientations, which is very important for optimizing the carrier concentration, regulating phonon scattering and thus enhancing the thermoelectric (TE) performance [146].

There are many papers reporting the hydrothermal synthesis of Bi_2Te_3 and its alloys, for which bismuth chloride ($BiCl_3$) and tellurium or tellurium dioxide (TeO_2) are used as the starting materials [147–153]. For example, Zhao et al. [153] synthesized Bi_2Te_3 nanotubes having diameters smaller than 100 nm and spiral tube-walls by conducting the hydrothermal synthesis at 150°C from the mixture precursors of $BiCl_3$ and Te in the solution of mixed NaOH, $NaBH_4$ and edetic acid (EDTA). They also found that the nanotubes could improve the *ZT* values of the Bi_2Te_3 based thermoelectric materials. Almost the similar hydrothermal method can be applied to the synthesis of PbTe only by replacing the starting materials from $BiCl_3$ to $PbCl_3$ [154]. It should be noted that the toxic and hazardous reducing agent such as N_2H_4 and $NaBH_4$ are used for the hydrothermal synthesis of

Bi_2Te_3 and PbTe, which may have environmental damages. To avoid this problem, Muramatsu et al. recently developed a green hydrothermal synthesis process using ascorbic acid in aqueous solution, in which ascorbic acid works not only as reducing agent but also as capping agent which has an excellent oxidation resistance [155]. It was reported that Bi_2Te_3 nanoparticles were successfully synthesized at high yields by their green method.

Solvothermal method is similar to the hydrothermal process, but its solvents or additives are usually organic compounds which contain both hydrophobic groups possessing an oil soluble component and hydrophilic groups presenting a water soluble component. In the aqueous phase, the hydrophobic groups can form the core of the aggregate but the hydrophilic groups contact with surrounding liquid, which can have an effect on the growth environments of target materials and then achieve the controllable fabrication of the various morphological TE composites under the optimal reaction conditions [156–158]. Although the solvothermal route has been demonstrated to provide excellent control over morphology, particle size and distribution [149,159], the problem is that the as-synthesized powders can be difficult to sinter, leading to low density, oxidation and the emergence of second phase. Besides, the organics can be easily adsorbed onto the surface of the nanocomposites during the precursor reaction procedures and post-washing from salts solvents. It is evident that high-efficiency thermoelectric nanomaterials will be synthesized and characterized from a much broader scope once the manipulation of some kinetic parameters, the knowledge of materials growth mechanism and post-treatment process are further integrated in the solvothermal method [160,161].

Recently, microwave-assisted hydrothermal or solvothermal method has received considerable attention as a promising method for the one-pot synthesis of large-scale TE nanostructures in solutions [160,162]. In general, microwave heating route is better than that in conventional water/oil-bath heating method mentioned above, when emphasizing the controllability of product's morphology and size as well as chemical uniformity in addition to processing efficiency [163,164]. As opposed to the traditional thermal heating, the understanding of microwave radiation for the activation of chemical reaction requires a certain physical principles. In recent years, various studies have been conducted to synthesize TE nanostructures using microwave (MW) heating route. For example, Li et al. [165] developed an ultra-fast microwave hydrothermal method, by which they synthesized SnTe particles with controlled sizes from micro-scale to nano-scale in a short period (20 min). The SPS-processed SnTe bulk materials made of 165 nm SnTe particles showed about 2.3 times *ZT* enhancement from its counterpart made of coarse powders synthesized by solid processing.

Although microwave heating has a clear advantage to assist the reaction, there are some challenges to be addressed [166,167]: 1) certain practical experiences on relevant parameters are required, because many publications do not provide essential reaction details, which results in poor connection from theoretical chemical synthesis to technical engineering sciences; 2) the accurate measurement of chemical reaction pressure and temperature are extremely problematic, which leads to speculations about nonthermal effects (hot spots and hot surfaces and supper-heating); 3) the controllable synthesis of complex systems has so far been proven to be a difficult task via MW-assisted solution technique, especially for the design and development of periodical heterogeneous TE nanosturctures. However, it is evident that further development of advanced MW radiation heating route will push the exploration forward.

Finally, the sol-gel method is also an important process which can be highly reproducible and scaled up to synthesize various nanosturctured thermoelectric materials in a wide range of compositions and shapes, including metal oxides, skutterudites and metal compositions [168,169]. It is possible to tailor the morphology affording the desired property in the sol-gel route, considering the controllable chemical reaction parameters, such as the nature of precursors, the use of surfactants, water/precursors/solvent ratios and washing/drying conditions [170]. The surfactant is largely used as a structure-shaped template to facilitate growth of the "targeted nanomaterials". Li et al. [171] employed the sol-gel method to synthesize $LaCo_{0.9}Ni_{0.1}O_{3-\delta}$ nanoparticles coated with $La_{0.9}Sr_{0.1}Co_{0.9}Ni_{0.1}O_{3-\delta}$ thin layers. Such a core-shell structured nanoparticles were partially retained to the corresponding bulk sample by normal sintering, resulting in grain boundaries composed of Sr/Ni-codoped $La_{0.9}Sr_{0.1}Co_{0.9}Ni_{0.1}O_{3-\delta}$ that act as a network with better electrical conductivity than the grains. As a result, a twofold enhancement in peak *ZT* near room temperature was achieved. This work showed that *ZT* can be enhanced using the sol-gel method by manipulating the local compositional distribution inside an individual particle. The representative works based on soft chemical reaction are illustrated in Table 3.

3 Sintering/consolidation processing

After the powders are synthesized or processed as discussed in Section 2, a proper sintering process is always needed to compact them, crystallize the grains, further purify and stabilize the main phase. After sintering under an appropriate condition (including both temperature, pressure and holding time), dense samples are obtained with good crystallinity and a fixed shape that are ready for characterization and measurements. In most cases, this is the last step for fabricating

Table 3 Representative works based on hydrothermal (HT) and solvothermal (ST) synthesis of thermoelectric materials

Type	Material	Method, ZT@T(K)	Reference
Bi-Te compounds	$(Bi, Sb)_2Te_3$	HT, 1.28@303 K	[153]
	$Bi_{2-x}Sb_xTe_3$	HT, 1.75@270 K	[151]
	$Bi_{0.5}Sb_{1.5}Te_3$	HT, 1.15@300 K	[162]
	$Bi_2Te_{3-x}Se_x$	HT, 1.23@480 K	[160]
	La-$Bi_2Se_{0.3}Te_{2.7}$	ST, 0.11@450 K	[172]
	Bi_2Te_3	ST, 0.6@600 K	[167]
	Te/Bi_2Te_3	ST, ~1@440 K	[173]
Tellurides	Sb_2Te_3	HT, 0.58@420 K	[174]
	S-Ag_2Te	ST, 0.62@550 K	[175]
	$AgPb_{10}BiTe_{12}$	ST, 0.46@570 K	[156]
	$Sn_xSb_2Te_{3+x}$	ST, 0.58@423 K	[176]
Sulfides/Selenides	SnSe	HT, 0.32@300 K	[146]
	SnSe	ST, 0.6@773 K	[157]
	SnS	ST, 0.25@773 K	[177]
	Ag-PbS	ST, 1.70@850 K	[161]
	$Cu_{12}Sb_4S_{13}$	ST, 0.85@720 K	[178]
Skutterudite	$Co_{1-x-y}Ni_xFe_ySb_3$	HT, 0.67@600 K	[151]
	$CoSb_3$	ST, 0.11@650 K	[179]

thermoelectric bulk materials, but sometimes post-treatment like annealing and hot-forging is carried out with specific motivations, which will be discussed in the next section. Here in this part we will introduce two techniques that are most widely used in sintering thermoelectric powders, i.e., spark plasma sintering (SPS) and hot pressing (HP), with a focus on their special features and the effects of sintering factors on the properties of thermoelectric materials. In addition, we will share some practical experiences in sintering some compounds using the two methods.

3.1 Spark plasma sintering

The rise of nanostructured thermoelectric materials over the past decades had also bought about a highlighted focus on the new sintering method, spark plasma sintering (SPS). An SPS system (SPS-211LX, Fuji Electronic Industrial Co., Ltd., Japan) is demonstrated in Figure 5(a) with the chamber and graphite die shown in the inset. The working principle of SPS is further depicted in Figure 5(b). An electrically conducting (usually made of graphite) die with powders loaded in between two punches is placed between graphite plates in the chamber that is subsequently evacuated. In order to realize a good electrical contact, graphite papers are inserted between the punch and the powder, between the plate and the electrode, and around the punch. By applying a direct current (DC) pulse power with a low voltage (several volts) and a large current (up to 1–10 kA) through the electrodes and the powder compacts, Joule heat is internally generated at a rate as high as 1000°C min^{-1}. Meanwhile, a uniaxial pressure (usually 10–100 MPa) is loaded to facilitate densification.

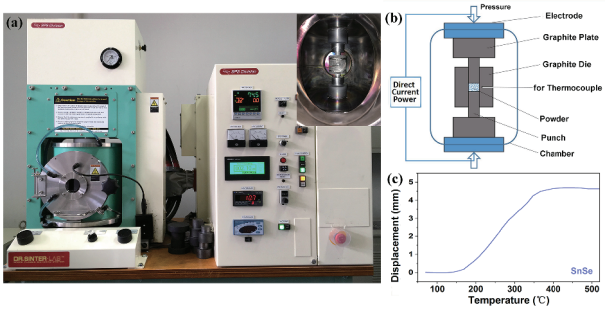

Figure 5 (Color online) (a) Photo of an SPS equipment (SPS-211LX, Fuji Electronic Industrial Co., Ltd., Japan) with the chamber and a graphite die (inset); (b) schematic depiction of an SPS system; (c) sintering curve for mechanically alloyed SnSe powders.

The history of SPS can be traced back to the early 1900s when a current-assisted sintering method was first mentioned [180]. A landmark occurred more than 60 a later. In 1966, Inoue invented and patented SPS in USA [181]. However, large implementation of SPS in industry did not come until 20 years later when Inoue's patent expired and various companies, mainly in Japan, started manufacturing and selling SPS systems. Thanks to the high heating rate, the sintering process can be accomplished within several minutes, thus retaining the nanostructures inherited from the quenched ingot and the fine grains of the powders synthesized by ball milling or chemical methods, which is often desired for designing high-performance thermoelectric materials with a low thermal conductivity. To some extent, the availability of SPS has boosted the outburst of nanostructured thermoelectric materials. Related studies are prevalent on

nearly all the well-known materials from a number of groups [9,22,63,78,182–190].

The sintering process involves the role and interplay of electrical field and current, pressure, heat and atmosphere etc [191]. The quality and properties of the samples depend strongly on these extrinsic factors.

3.1.1 Electrical current and field

Since almost all the known thermoelectric materials are semiconductors with a decent electrical conductivity, the density of current that directly flows through the sample is appreciable [192]. In this case, various types of interactions between current and the powders are present, among which we focus on the one related to Peltier effect that is nontrivial for thermoelectric materials [193]. As shown in Figure 6(a), if the sample is a p-type semiconductor, it takes energy for the electrical field to "pull" a hole carrier from the anode to the sample, which is against the "force" of carrier concentration gradient, thus cooling the anode. As the hole meets the cathode, it tends to be "pushed" by the concentration gradient to the cathode, thus heating it. It goes the similar way for n-type semiconductors as shown in Figure 6(b). This effect brings about local variation of heat and the consequential temperature distribution. A typical and straightforward consequence of Peltier effect is that the SPSed pellet exhibits a large difference in grain size and electrical conductivity between the top and the down sides. At this stage, AC-activated SPS seems not available yet to solve the above problem. Instead, we recently found that re-sintering a sample from an opposite direction will help eliminate the inhomogeneity in LAST materials.

In addition to the Peltier effect, the current and field themselves may cause migration of elements in the newly appearing ionic thermoelectric materials. A typical representative is $Cu_{2-x}Q$ (Q = S, Se, Te) compounds in which the anions form a grid lattice while the Cu atom tends to jump from one site to one vacancy, exhibiting a liquid-like conduction behavior [194]. Meng et al. [195] observed an obvious migration of copper after SPS and ZEM-measurement. However, this issue has not been widely addressed in relevant studies on these compounds.

3.1.2 Heat and temperature

A homogeneous and steady heat flow is always required for sintering but never possible. In addition to the Peltier effect as discussed above, for thermoelectric materials, heat conduction may be also hindered, more or less, by the low thermal conductivity. Severe impacts like cracks are likely to occur especially when cooled very fast. In the case of $Cu_{12}Sb_4S_{13}$ compounds, only with a controlled cooling rate < 15°C min^{-1} could we obtain a good sample without cracks. Another example is even extreme: Cu_3SbSe_3, a compound with κ < 0.5 W mK^{-1} can be hardly sintered by SPS [97]; instead, a hot pressing method is needed to obtain the pure phase and high-quality samples. The exact reasons for the difficulty in sintering the two materials are not clear yet, but the low thermal conductivity and possible abnormal behavior of Cu atoms (order-disorder transition and/or ionic motion) are likely to be at play [196,197].

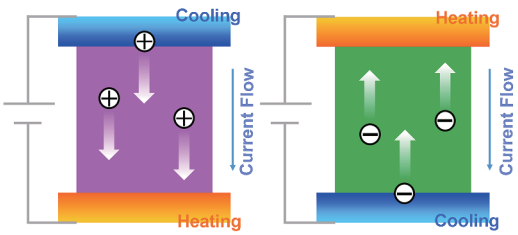

Figure 6 (Color online) Peltier effect in p- and n-type semiconductors.

The other concern is the temperature measurement. Usually when lower than 800°C–900°C, the temperature is detected by a thermocouple (TC, commonly K-type) that is inserted into a hole in the die (Figure 5(a) and (b)). Then the following factors significantly affect the accuracy of temperature measurement. One is the relative position of the powders and the hole; ideally, the hole should be at the central part of the powders. Another one is the position of TC in the hole. If they are just loosely contacted, TC can jump out from the hole when large displacement occurs during heating. Finally, contamination of TC and possible reaction between TC and the die should be considered. If the sintering temperature is higher than 800°C–900°C, an external optical pyrometer, usually infrared thermometer, will be employed. In this case, great attention should also be paid to the positioning and focusing of the detector.

3.1.3 Pressure and displacement

In most cases of SPS, a uniaxial pressure is loaded onto the punches of the die to ensure good densification of the powders. Normally, the pressure is below 100 MPa for graphite dies and can go beyond this value for dies made of steel or tungsten carbide alloys. Figure 5(c) is a typical sintering curve of mechanically alloyed SnSe powders. Positive value of displacement means shrinkage of the sample, negative expansion. The curve roughly reflects three processes during sintering. From room temperature to 130°C, there is no shrinkage of the powder compact, even with a little expansion due to heating. When the temperature exceeds 130°C, the sintering process starts as featured by a rapid densification of the powder compact that is governed by the grain boundary diffusion and the crystallization of the grains. Densification ends at around 400°C followed by a thermal expansion.

The value and the way of pressurizing will influence the microstructure of the samples. Usually a preload is needed to promote contact and densification before sintering starts. In some special cases, such as texture engineering, a relatively small preload may be favorable for facilitating the re-

arrangement and deformation of the grains. When reaching the holding period, full load should be applied. The holding temperature is usually set 50°C–100°C higher than the one when shrinkage ends to ensure full densification and also avoid overheating. Of course, the operation temperature and other factors such as possible phase transitions should also be considered when designing a sintering program. After sintering, the pressure should be gradually removed since a sudden stop unloading is likely to cause cracks in the sample subjected to cooling down.

Although SPS has been proved repeatedly to be an efficient sintering method for thermoelectric materials, its shortcomings are also evident. SPS gets popular for its high heating rate, but in turn such short sintering time can fail to ensure the stability of the sample, especially for those mechanically alloyed or chemically synthesized fine powders with a high chemical reactivity, abundant defects and secondary phases. Remaining chemical reaction, severe thermal deformation, chemical/thermal decomposition and volatilization frequently occur during high-temperature measurement on these samples. Sometimes post treatment like long-time annealing is employed to promote complete chemical reaction of the constituents, eliminate second phases and diminish crystal defects and strains, which will be discussed in Section 4.2.

3.2 Hot pressing

Featured by simultaneous application of heat and pressure, hot pressing (HP) is well used for powder compacts at a high temperature under which sintering and creep processes are induced. HP was developed primarily to sinter hard and brittle powders that are usually difficult to be sintered by normal sintering or pressureless sintering, and now this technique is being widely employed in sintering various thermoelectric materials as well. As compared to SPS, the heating rate of HP is lower than SPS, and a longer holding time (usually from half to several hours) is needed, so enhanced homogeneity in density, structure and composition can be obtained by HP with a better processing stability.

Two heating modes are commonly seen in HP: inductive heating and convective heating (or indirect resistance heating). In the former one, heat is produced within the die that is placed in an induction coil and subjected to a high-frequency electromagnetic field. Simultaneously, uniaxial pressure is applied onto the punches. An advantage for this type of heating is that the heating rate can be very high. However, it is difficult to realize a uniform distribution of heat since the mold should be placed very exactly at the center of the coil and the heating process depends strongly on the coupling effect and the thermal conductivity of the mold. High-performance lead chalcogenides [23], skutterudites [8] and Zintl compounds [198] have been developed using induction HP from Snyder's group at Caltech and Northwestern University.

Convective heating is commonly employed in a furnace box. In this type of HP, the die is placed in a chamber embedded with heating elements that are heated by electric current. In this case, heating process is relatively independent of the conductivity and position of the mold. Uniform and steady heating can be achieved given enough time. Nonetheless, the time may be rather long for sufficient heat transfer from the heating elements to chamber atmosphere, to the surface of the die, and finally to the powders. Recently, single-phase Cu_3SbSe_3 bulk samples were fabricated using convection HP [97], whose *ZT* is twice as high as previously reported values [199], but it was found difficult to sinter this compound by SPS.

4 Nanostructuring post-treatment

Nanostructuring has been found effective to strengthen the scattering of phonons and reduce the thermal conductivity [19,22,112]. However, the transport of carriers is sometimes also undesirably deteriorated by the nanostructures, hence resulting in a limited improvement of the thermoelectric performance [29]. In order to maximally enhance the thermoelectric performance, nanostructuring post-treatment has been introduced, showing satisfactory results. The main target of nanostructuring post-treatment is to minimize the nanostructures' scattering on charged carriers, while remaining the low thermal conductivity. This is possible when the size of the nanostructure is larger than the mean free path of the carriers but smaller than that of the phonons. Herein, we focus on two ways for the post-treatment: one is texture processing by "hot forging" that is usually applied to anisotropic thermoelectric materials; the other is annealing to promote homogeneity and stability, also to incur the formation of *in situ* nanostructures.

4.1 Hot forging

For anisotropic thermoelectric materials like Bi_2Te_3-based alloys [200] and BiCuSeO [201] compounds, the in-plane (perpendicular to the long axis) electrical conductivity is usually much higher than other directions due to stronger chemical bonding, hence in-plane grain alignment should be advantageous for electrical transport properties. With advanced powder processing methods, researchers have been trying to combine the texture structure and the nanostructures together for simultaneously increasing electrical conductivity and decreasing the thermal conductivity [21,78,202,203]. Hot-forging has been widely demonstrated to be able to align the grains and construct a highly texture structure [202,204–206], and thus result in an enhanced carrier mobility. It should be noted that texture-enhanced electrical conductivity can result in an increase of electron thermal conductivity. On the other hand, for many anisotropic materials, the in-plane phonons transport is intrinsically faster than the out-of-plane, thus grain alignment may also

increase the lattice thermal conductivity. Hence the total thermal conductivity can be also increased by hot-forging at the same time when we attempt to enhance the electrical conductivity, but it is still worth trying as long as the rise of electrical conductivity outweighs thermal conductivity. Moreover, although the overall grain size would be somehow increased after hot forging, the parental nanocrystalline may be partially retained [202]. More importantly, new nanostructures can form during the hot-forging process under repeated mechanical deformation [203]. The nanostructures with different sizes formed during hot-forging are effective to scatter the broad-wavelength phonons and decrease the thermal conductivity. In this way, the scattering of phonons by nanostructures may be still effective while the transport of charge carriers can also benefit from the texture structure.

Figure 7 schematically shows the hot forging process. Firstly, a long cylinder bulk is sintered from fine powders. The grains of a sintered bulk are small and relatively in an isotropic distribution. Then the bulk is subjected to further sintering process in a larger die with more space to be squeezed in the diameter direction. After several times mechanical alignment under compression, the texture structure forms along the direction perpendicular to the pressing direction accompanied with grains growth. As an effective and practicable texture constructing method to enhance the electrical conductivity, hot forging has been explored in several thermoelectric materials. For instance, Mikami et al. [205] applied hot forging in $Ca_3Co_4O_9$ and hence largely enhanced the electrical conductivity as well as *ZT*. Sui et al. [201] also reported a maximum *ZT* of 1.4 for $Bi_{0.875}Ba_{0.125}CuSeO$ benefit from hot forging, which is much higher than 1.1 for the non-textured samples. Furthermore, hot forging could also decrease the thermal conductivity while enhancing the electrical properties at the same time in some materials. Aforementioned, the repeated mechanical deformation process can lead to the formation of some nanostructures and thus decrease the thermal conductivity. In 2010, Shen et al. [203] reported that recrystallization happens during hot forging, resulting in many *in situ* nanostructures. Such nanostructures strengthen the scattering of phonons and thus decrease the thermal conductivity. Therefore, a maximum $ZT > 1.3$ has been achieved in BiSbTe, due to the increased power factor as well as the reduced thermal conductivity. In 2014, Jiang et al. [202] also found that hot forging could lower the thermal conductivity of p-type BiSbTe alloys and also enhance the Seebeck coefficient. In 2016, Pan et al. [78] reported that by optimizing the hot forging temperature, the texture degree, the amount and size of the nanostructures could be well controlled, resulting in a maximum ratio of the electrical conductivity to thermal conductivity. Consequently, the texture structure advantages the transport of charge carriers while the nanostructures and

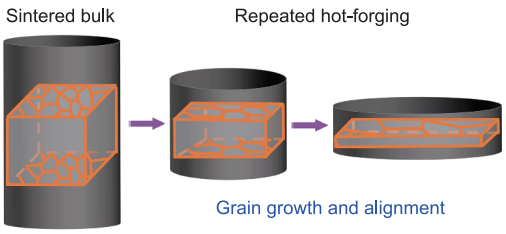

Figure 7 (Color online) Schematic plot of the hot-forging process. Grain growth and alignment occurs after repeated hot-forging.

crystal defects effectively scatter the phonons, resulting in a high *ZT* of 1.1 for n-type BiTeSe alloys.

On the other hand, there is also a top-down method that has similar effects (combining texture and nanostructures together) like hot forging, in which the zone-melting ingots are directly compacted at high temperatures under pressure. As reported by Hu et al. [21], by directly hot pressing the commercial ingots, coarse grains of the ingots are broken and texture degree is somewhat decreased. It is found that many nanograins or nanoscale defects would form during the process, being helpful to scatter the phonons and decrease the thermal conductivity. A high *ZT* of 1.2 was finally achieved in n-type BiTeSe alloys, because of the synergistic combination of reduced lattice thermal conductivity and maintained high power factor.

It is noted that in addition to texture engineering and nanostructuring, both bottom-up hot forging and top-down hot deformation have more complex effects in Bi_2Te_3-based compounds. For example, they could also introduce antisite defects and donor-like effect that strongly change the carrier concentration and thus modify the electrical properties [41,78]. In addition, the point defects also act as scattering centers for both charge carriers and phonons, result in decreased mobility and thermal conductivity [21].

4.2 Annealing (including repeated MA-SPS)

For most of the materials, annealing can reduce or eliminate the defects, impurities and inhomogeneities in the matrix, as shown in Figure 8(a)–(d) [207], leading to an enhancement of the electrical transport properties. Interestingly, annealing may also introduce a second phase nanoscopic precipitates in the matrix (Figure 8(e)–(h) [207]), which can significantly intensify the scattering of phonons and thus decrease the thermal conductivity. One of the most significant effect of annealing is to enhance the microscopic homogeneity, degree of crystallinity and phase purity, thus maintaining or enhancing the carrier mobility and electrical properties. In 1962, Schultz et al. [208] reported that annealing in an inert atmosphere made the heavily deformed Bi_2Te_3 samples exhibit the properties similar to those of carefully grown single crystals. During annealing, Te vacancies would migrate slowly

which allows dislocations to climb into stable positions. For an enough long time annealing, dislocation array formation, recrystallization and grain growth lead to a total annihilation of vacancies and thus increase the carrier mobility. Moreover, the carrier concentration is also affected due to the decreased charged Te vacancies. In 2003, Yamashita et al. [207] studied the annealing effect on the thermoelectric properties of both p- and n-type Bi_2Te_3-based alloys. It was found that the second phase disappears and the composition become more uniform after annealing 10 h at 673 K in vacuum, as shown in Figure 8(a)–(d). Consequently, high *ZT* values of 1.26 and 1.19 for p- and n-type Bi_2Te_3-based alloys were achieved. However, the reasons are reserved and need further exploration. Nevertheless, it should be kept in mind that how to control the microstructure and chemical composition after annealing would be important for the enhancement of *ZT* values, which all strongly depend on the annealing temperature, time as well as the atmosphere. This is more complicated if there is a great change of charged point defects in the samples during annealing. In 2009, Zhao et al. [209] reported a power factor enhancement in Bi_2Te_3 by annealing at low temperatures. It was pointed out that when annealing temperature was above 523 K, the electrical performances were reduced because of the volatilization of Te, leading to more anion vacancies (positive charged) in the matrix. In 2013, Schumacher et al. [210] reported that annealing in Te atmosphere could strongly improve the chemical composition, charge carrier density and mobility of Bi_2Te_3-based films, due to the equilibrium chemical conditions. It was demonstrated that the stepwise improvements of the crystal structure could lead to the improvements in thermoelectric parameters.

On the other hand, annealing can also be employed to decrease the thermal conductivity by introducing nanoscopic precipitates. There is one representative work that includes almost all the effects of annealing: enhancement of carrier mobility through improving the crystalline quality, optimization of the carrier concentration benefiting from composition homogenization, and reduction of thermal conductivity by nanoprecipitates. This work based on $AgPb_mSbTe_{m+2}$ (LAST) compound was published in 2008 by Zhou et al. [211]. A high *ZT* of 1.5 has been achieved via an appropriate annealing treatment after MA and SPS. The mobility is largely enhanced and the carrier concentration is decreased due to the volatilization of Pb. Moreover, the thermal conductivity is also reduced at the same time, which is ascribed to the nanoscopic inhomogeneities induced by the annealing. As shown in Figure 8(e)–(h), the annealed samples display large nanoscopic regions, whereas it should be noted that the nanostructures in the unannealed sample are due to the compositional fluctuations as they are coherent with their surrounding crystal matrix. It should be mentioned that such effects can also be realized in repeated BM and SPS. In 2014, Li et al. [102] revealed that by repeating the BM and SPS process, large (50%) enhancement of *ZT* was achieved in nanostructured $AgPb_mSbTe_{m+2}$ (LAST). It was found that repeated BM process could effectively increase the electrical conductivity and thermopower while also reducing the thermal conductivity due to the reduction of grain sizes, formation of nanoprecipitates, and elimination of excessive Pb nanodispersions.

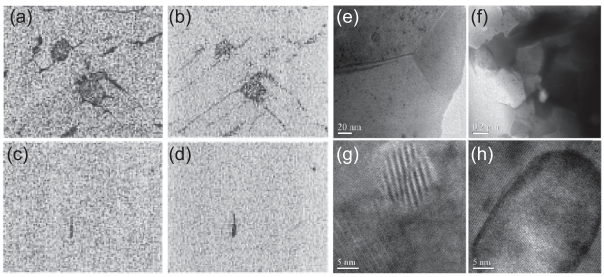

Figure 8 EPMA micrographs of (a), (c) Bi and (b), (d) Te elements of Bi_2Te_3-based alloys: (a), (b) Before annealing; (c), (d) after annealing at 673 K for 10 h in vacuum. Microstructures are more uniform after annealing. (e), (f) TEM images and (g), (h) HRTEM images of unannealed and annealed $AgPb_mSbTe_{m+2}$ samples: (e), (g) Unannealed sample and (f), (h) the sample annealed for 30 d. Nanoscopic precipitates show up after annealing. (a)–(d) are the reproduction from ref. [207], the Japan Society of Applied Physics. (e)–(h) are reprinted with permission from ref. [211], American Chemical Society.

5 Summary and perspective

In this article, we have reviewed and summarized the processing aspects of thermoelectric materials with three focuses on the powder synthesis, advanced sintering process and the formation of nanostructures in bulk materials. It is well known that fine-grained and nano-composite structures usually lead to a high thermoelectric performance, so the synthesis of fine or nano-sized particles of a targeted compound with designed compositions is important. As described above, high-energy ball milling or so-called mechanical alloying is a convenient method, which can be conducted in research laboratories and easily scaled up in industries. In some cases, to enhance the compositional homogeneity and/or obtain fine particles, thermoelectric compounds are firstly synthesized by a melting process (including melt-spinning), and the resultant products are then pulverized by further ball milling. Of course, soft chemical reaction methods are more suitable for the synthesis of nanoparticles with controllable sizes and morphology, but they are less reviewed because of its complexity as compared with the physical methods.

SPS is increasingly used for making thermoelectric bulk materials, as a rapid sintering process with clear advantages of lower sintering temperature and short holding times. Also importantly, most thermoelectric materials must be sintered in a reduced atmosphere, which can be easily realized in SPS that is conducted in vacuum. Additionally, SPS can effectively suppress the grain growth by rapid heating and low-

temperature sintering, which is very important especially for some cases where the morphology of the synthesized powders is desired to be retained during the sintering process. It is known that nanoscopic precipitates are beneficial to the reduction of thermal conductivity, and it is often experienced that nanoscopic precipitates often appear in many SPS-processed thermoelectric materials, whose formation may be related to the applications of pulsed current to the semiconducting materials, but it needs more studies to uncover the formation mechanisms. Notably, annealing processes are also intentionally conducted to create such nanocomposite structures. Besides, SPS can also be used as a texturing process as done by hot pressing or hot forging when a larger die is used following the first step for consolidation.

In summary, the state-of-the-art thermoelectric materials are mostly fabricated by modified powder metallurgical processes, in which fine-grained microstructures with controlled nanostructures can be more easily obtained. Nevertheless, more and more studies are still required to develop new processes leading to favorable microstructures for further *ZT* enhancement, which are also suitable for mass production.

This work was supported by the National Natural Science Foundation of China (Grant No. 11474176) and the Ministry of Science and Technology of China (Grant No. 2013CB632503).

1 DiSalvo F J. Thermoelectric cooling and power generation. Science, 1999, 285: 703–706
2 Bell L E. Cooling, heating, generating power, and recovering waste heat with thermoelectric systems. Science, 2008, 321: 1457–1461
3 Chen L G, Meng F K, Sun F R. Thermodynamic analyses and optimization for thermoelectric devices: The state of the arts. Sci China Tech Sci, 2016, 59: 442–455
4 Snyder G J, Toberer E S. Complex thermoelectric materials. Nat Mater, 2008, 7: 105–114
5 Heremans J P. Thermoelectricity: The ugly duckling. Nature, 2014, 508: 327–328
6 Zhang X, Zhao L D. Thermoelectric materials: Energy conversion between heat and electricity. J Mater, 2015, 1: 92–105
7 Vineis C J, Shakouri A, Majumdar A, et al. Nanostructured thermoelectrics: Big efficiency gains from small features. Adv Mater, 2010, 22: 3970–3980
8 Tang Y, Gibbs Z M, Agapito L A, et al. Convergence of multi-valley bands as the electronic origin of high thermoelectric performance in $CoSb_3$ skutterudites. Nat Mater, 2015, 14: 1223–1228
9 Wang S, Yang J, Wu L, et al. On intensifying carrier impurity scattering to enhance thermoelectric performance in Cr-doped $Ce_yCo_4Sb_{12}$. Adv Funct Mater, 2015, 25: 6660–6670
10 Zhu T, Fu C, Xie H, et al. High efficiency half-heusler thermoelectric materials for energy harvesting. Adv Eng Mater, 2015, 5: 1500588
11 Fu C, Bai S, Liu Y, et al. Realizing high figure of merit in heavy-band p-type half-Heusler thermoelectric materials. Nat Commun, 2015, 6: 8144
12 Chung D Y, Hogan T, Brazis P, et al. $CsBi_4Te_6$: A high-performance thermoelectric material for low-temperature applications. Science, 2000, 287: 1024–1027
13 Shi X, Yang J, Bai S, et al. On the design of high-efficiency thermoelectric clathrates through a systematic cross-substitution of framework elements. Adv Funct Mater, 2010, 20: 755–763
14 Zhao L D, Lo S H, Zhang Y, et al. Ultralow thermal conductivity and high thermoelectric figure of merit in SnSe crystals. Nature, 2014, 508: 373–377
15 Duong A T, Nguyen V Q, Duvjir G, et al. Achieving $ZT = 2.2$ with Bi-doped n-type SnSe single crystals. Nat Commun, 2016, 7: 13713
16 Zhao L L, Wang X L, Wang J Y, et al. Superior intrinsic thermoelectric performance with zT of 1.8 in single-crystal and melt-quenched highly dense $Cu_{2-x}Se$ bulks. Sci Rep, 2015, 5: 7671
17 Zhao L D, Tan G, Hao S, et al. Ultrahigh power factor and thermoelectric performance in hole-doped single-crystal SnSe. Science, 2016, 351: 141–144
18 Peng K, Lu X, Zhan H, et al. Broad temperature plateau for high *ZT*s in heavily doped p-type SnSe single crystals. Energ Environ Sci, 2016, 9: 454–460
19 Poudel B, Hao Q, Ma Y, et al. High-thermoelectric performance of nanostructured bismuth antimony telluride bulk alloys. Science, 2008, 320: 634–638
20 Kim S I, Lee K H, Mun H A, et al. Dense dislocation arrays embedded in grain boundaries for high-performance bulk thermoelectrics. Science, 2015, 348: 109–114
21 Hu L, Wu H, Zhu T, et al. Tuning multiscale microstructures to enhance thermoelectric performance of n-type bismuth-telluride-based solid solutions. Adv Eng Mater, 2015, 5: 1500411
22 Biswas K, He J, Blum I D, et al. High-performance bulk thermoelectrics with all-scale hierarchical architectures. Nature, 2012, 489: 414–418
23 Pei Y, Shi X, LaLonde A, et al. Convergence of electronic bands for high performance bulk thermoelectrics. Nature, 2011, 473: 66–69
24 Wu H J, Zhao L D, Zheng F S, et al. Broad temperature plateau for thermoelectric figure of merit $ZT > 2$ in phase-separated $PbTe_{0.7}S_{0.3}$. Nat Commun, 2014, 5: 4515
25 Rowe D M. CRC Handbook of Thermoelectrics. London: CRC Press, 1995
26 Ainsworth L. Single crystal bismuth telluride. Proc Phys Soc B, 1956, 69: 606–612
27 Fleurial J P, Gailliard L, Triboulet R, et al. Thermal properties of high quality single crystals of bismuth telluride—Part I: Experimental characterization. J Phys Chem Solids, 1988, 49: 1237–1247
28 Zheng Y, Zhang Q, Su X, et al. Mechanically robust BiSbTe alloys with superior thermoelectric performance: A case study of stable hierarchical nanostructured thermoelectric materials. Adv Eng Mater, 2015, 5: 1401391
29 Pan Y, Wei T R, Cao Q, et al. Mechanically enhanced p- and n-type Bi_2Te_3-based thermoelectric materials reprocessed from commercial ingots by ball milling and spark plasma sintering. Mater Sci Eng B, 2015, 197: 75–81
30 Li J F, Liu W S, Zhao L D, et al. High-performance nanostructured thermoelectric materials. NPG Asia Mater, 2010, 2: 152–158
31 Sootsman J R, Chung D Y, Kanatzidis M G. New and old concepts in thermoelectric materials. Angew Chem Int Ed, 2009, 48: 8616–8639
32 Yang J, Yip H L, Jen A K Y. Rational design of advanced thermoelectric materials. Adv Eng Mater, 2013, 3: 549–565
33 Zebarjadi M, Esfarjani K, Dresselhaus M S, et al. Perspectives on thermoelectrics: From fundamentals to device applications. Energ Environ Sci, 2012, 5: 5147–5162
34 Zhu T, Liu Y, Fu C, et al. Compromise and synergy in high-efficiency thermoelectric materials. Adv Mater, 2017, 29: 1605884
35 Zeier W G, Zevalkink A, Gibbs Z M, et al. Thinking like a chemist: Intuition in thermoelectric materials. Angew Chem Int Ed, 2016, 55: 6826–6841
36 Pichanusakorn P, Bandaru P. Nanostructured thermoelectrics. Mat Sci Eng R, 2010, 67: 19–63
37 Su X, Fu F, Yan Y, et al. Self-propagating high-temperature synthesis for compound thermoelectrics and new criterion for combustion processing. Nat Commun, 2014, 5: 4908
38 Chen W C, Wu Y C, Hwang W S, et al. A numerical study of zone-

melting process for the thermoelectric material of Bi_2Te_3. IOP Conf Ser Mater Sci Eng, 2015, 84: 012094
39 Kanatzidis M G. Nanostructured thermoelectrics: The new paradigm? Chem Mater, 2010, 22: 648–659
40 Wu D, Zhao L D, Tong X, et al. Superior thermoelectric performance in PbTe–PbS pseudo-binary: Extremely low thermal conductivity and modulated carrier concentration. Energ Environ Sci, 2015, 8: 2056–2068
41 Hu L, Zhu T, Liu X, et al. Point defect engineering of high-performance bismuth-telluride-based thermoelectric materials. Adv Funct Mater, 2014, 24: 5211–5218
42 Hsu K F, Loo S, Guo F, et al. Cubic $AgPb_mSbTe_{2+m}$: Bulk thermoelectric materials with high figure of merit. Science, 2004, 303: 818–821
43 Heremans J P, Jovovic V, Toberer E S, et al. Enhancement of thermoelectric efficiency in PbTe by distortion of the electronic density of states. Science, 2008, 321: 554–557
44 Pei Y, LaLonde A, Iwanaga S, et al. High thermoelectric figure of merit in heavy hole dominated PbTe. Energ Environ Sci, 2011, 4: 2085
45 Wang H, Pei Y, LaLonde A D, et al. Heavily doped p-type PbSe with high thermoelectric performance: An alternative for PbTe. Adv Mater, 2011, 23: 1366–1370
46 Wang H, Schechtel E, Pei Y, et al. High thermoelectric efficiency of n-type PbS. Adv Energ Mater, 2013, 3: 488–495
47 Liu H, Yuan X, Lu P, et al. Ultrahigh thermoelectric performance by electron and phonon critical scattering in $Cu_2Se_{1-x}I_x$. Adv Mater, 2013, 25: 6607–6612
48 He Y, Day T, Zhang T, et al. High thermoelectric performance in non-toxic earth-abundant copper sulfide. Adv Mater, 2014, 26: 3974–3978
49 Zhang Q, Chere E K, Sun J, et al. Studies on thermoelectric properties of n-type polycrystalline $SnSe_{1-x}S_x$ by iodine doping. Adv Eng Mater, 2015, 5: 1500360
50 Chen C L, Wang H, Chen Y Y, et al. Thermoelectric properties of p-type polycrystalline SnSe doped with Ag. J Mater Chem A, 2014, 2: 11171
51 Wu H, Chang C, Feng D, et al. Synergistically optimized electrical and thermal transport properties of SnTe via alloying high-solubility MnTe. Energ Environ Sci, 2015, 8: 3298–3312
52 Liu X, Zhu T, Wang H, et al. Low electron scattering potentials in high performance $Mg_2Si_{0.45}Sn_{0.55}$ based thermoelectric solid solutions with band convergence. Adv Eng Mater, 2013, 3: 1238–1244
53 Chen X, Girard S N, Meng F, et al. Approaching the minimum thermal conductivity in rhenium-substituted higher manganese silicides. Adv Eng Mater, 2014, 4: 1400452
54 Yang C, Huang F, Wu L, et al. New stannite-like p-type thermoelectric material Cu_3SbSe_4. J Phys D: Appl Phys, 2011, 44: 295404
55 Lai W, Wang Y, Morelli D T, et al. From bonding asymmetry to anharmonic rattling in $Cu_{12}Sb_4S_{13}$ tetrahedrites: When lone-pair electrons are not so lonely. Adv Funct Mater, 2015, 25: 3648–3657
56 Rudnev V. Handbook of Induction Heating. 2nd ed. Boca Raton: CRC Press, 2014
57 Shi X, Yang J, Salvador J R, et al. Multiple-filled skutterudites: High thermoelectric figure of merit through separately optimizing electrical and thermal transports. J Am Chem Soc, 2011, 133: 7837–7846
58 Salvador J R, Shi X, Yang J, et al. Synthesis and transport properties of $M_3Ni_3Sb_4$ (MZr and Hf): An intermetallic semiconductor. Phys Rev B, 2008, 77: 235217
59 Moss A R. Arc-melting processes for the refractory metals. J Less Common Met, 1959, 1: 60–72
60 Yan X, Joshi G, Liu W, et al. Enhanced thermoelectric figure of merit of p-type half-heuslers. Nano Lett, 2011, 11: 556–560
61 Yamashita O, Sadatomi N. Thermoelectric properties of $Si_{1-x}Ge_x$ ($x \leqslant 0.10$) with alloy and dopant segregations. J Appl Phys, 2000, 88: 245–251
62 Fu C, Zhu T, Liu Y, et al. Band engineering of high performance p-type FeNbSb based half-Heusler thermoelectric materials for figure of merit $zT > 1$. Energ Environ Sci, 2015, 8: 216–220
63 Yu C, Zhu T J, Shi R Z, et al. High-performance half-Heusler thermoelectric materials $Hf_{1-x}Zr_xNiSn_{1-y}Sb_y$ prepared by levitation melting and spark plasma sintering. Acta Mater, 2009, 57: 2757–2764
64 Suryanarayana C, Ivanov E, Boldyrev V V. The science and technology of mechanical alloying. Mater Sci Eng A, 2001, 304-306: 151–158
65 Liu J, Li J F. Bi_2Te_3 and Bi_2Te_3/Nano-SiC prepared by mechanical alloying and spark plasma sintering. Key Eng Mater, 2005, 280-283: 397–400
66 Ma Y, Hao Q, Poudel B, et al. Enhanced thermoelectric figure-of-merit in p-type nanostructured bismuth antimony tellurium alloys made from elemental chunks. Nano Lett, 2008, 8: 2580–2584
67 Pan Y, Wei T R, Wu C F, et al. Electrical and thermal transport properties of spark plasma sintered n-type $Bi_2Te_{3-x}Se_x$ alloys: The combined effect of point defect and Se content. J Mater Chem C, 2015, 3: 10583–10589
68 Wu C F, Wei T R, Li J F. Electrical and thermal transport properties of $Pb_{1-x}Sn_x$ Se solid solution thermoelectric materials. Phys Chem Chem Phys, 2015, 17: 13006–13012
69 Yu B, Zhang Q, Wang H, et al. Thermoelectric property studies on thallium-doped lead telluride prepared by ball milling and hot pressing. J Appl Phys, 2010, 108: 016104
70 Yang J Y, Aizawa T, Yamamoto A, et al. Thermoelectric properties of n-type $(Bi_2Se_3)_x(Bi_2Te_3)_{1-x}$ prepared by bulk mechanical alloying and hot pressing. J Alloys Compd, 2000, 312: 326–330
71 Bouad N, Marin-Ayral R M, Tédenac J C. Mechanical alloying and sintering of lead telluride. J Alloys Compd, 2000, 297: 312–318
72 Schilz J, Riffel M, Pixius K, et al. Synthesis of thermoelectric materials by mechanical alloying in planetary ball mills. Powder Tech, 1999, 105: 149–154
73 Li J, Tan Q, Li J F, et al. BiSbTe-Based nanocomposites with high *ZT*: The effect of SiC nanodispersion on thermoelectric properties. Adv Funct Mater, 2013, 23: 4317–4323
74 Itô M, Tada T, Katsuyama S. Thermoelectric properties of $Fe_{0.98}Co_{0.02}Si_2$ with ZrO_2 and rare-earth oxide dispersion by mechanical alloying. J Alloys Compd, 2003, 350: 296–302
75 Chen S, Lukas K C, Liu W, et al. Effect of Hf concentration on thermoelectric properties of nanostructured n-type half-heusler materials $Hf_xZr_{1-x}NiSn_{0.99}Sb_{0.01}$. Adv Eng Mater, 2013, 3: 1210–1214
76 Joshi G, Lee H, Lan Y, et al. Enhanced thermoelectric figure-of-merit in nanostructured p-type silicon Germanium bulk alloys. Nano Lett, 2008, 8: 4670–4674
77 Wang X W, Lee H, Lan Y C, et al. Enhanced thermoelectric figure of merit in nanostructured n-type silicon germanium bulk alloy. Appl Phys Lett, 2008, 93: 193121
78 Pan Y, Li J F. Thermoelectric performance enhancement in n-type $Bi_2(TeSe)_3$ alloys owing to nanoscale inhomogeneity combined with a spark plasma-textured microstructure. NPG Asia Mater, 2016, 8: e275
79 Starý Z, Horák J, Stordeur M, et al. Antisite defects in $Sb_{2-x}Bi_xTe_3$ mixed crystals. J Phys Chem Solids, 1988, 49: 29–34
80 Navrátil J, Starý Z, Plecháček T. Thermoelectric properties of p-type antimony bismuth telluride alloys prepared by cold pressing. Mater Res Bull, 1996, 31: 1559–1566
81 Liu W S, Zhang Q, Lan Y, et al. Thermoelectric property studies on Cu-doped n-type $Cu_xBi_2Te_{2.7}Se_{0.3}$ nanocomposites. Adv Eng Mater, 2011, 1: 577–587
82 Li F, Li J F, Zhao L D, et al. Polycrystalline BiCuSeO oxide as a potential thermoelectric material. Energ Environ Sci, 2012, 5: 7188–7195
83 Wei T R, Wu C F, Zhang X, et al. Thermoelectric transport properties of pristine and Na-doped $SnSe_{1-x}Te_x$ polycrystals. Phys Chem Chem Phys, 2015, 17: 30102–30109
84 Martin-Lopez R, Lenoir B, Dauscher A, et al. Preparation of n-type Bi–Sb–Te thermoelectric material by mechanical alloying. Solid State

Commun, 1998, 108: 285–288
85 Chen X, Shi L, Zhou J, et al. Effects of ball milling on microstructures and thermoelectric properties of higher manganese silicides. J Alloys Compd, 2015, 641: 30–36
86 Ge Z H, Zhang B P, Chen Y X, et al. Synthesis and transport property of $Cu_{1.8}S$ as a promising thermoelectric compound. Chem Commun, 2011, 47: 12697–12699
87 Itoh T, Yamada M. Synthesis of thermoelectric manganese silicide by mechanical alloying and pulse discharge sintering. J Elec Mater, 2009, 38: 925–929
88 Li J, Tan Q, Li J F. Synthesis and property evaluation of $CuFeS_{2-x}$ as earth-abundant and environmentally-friendly thermoelectric materials. J Alloys Compd, 2013, 551: 143–149
89 Liu W, Kim H S, Chen S, et al. n-Type thermoelectric material $Mg_2Sn_{0.75}Ge_{0.25}$ for high power generation. Proc Natl Acad Sci USA, 2015, 112: 3269–3274
90 Shin D K, Jang K W, Ur S C, et al. Thermoelectric properties of higher manganese silicides prepared by mechanical alloying and hot pressing. J Elec Mater, 2013, 42: 1756–1761
91 Wang H, Li J F, Nan C W, et al. High-performance $Ag_{0.8}Pb_{18+x}SbTe_{20}$ thermoelectric bulk materials fabricated by mechanical alloying and spark plasma sintering. Appl Phys Lett, 2006, 88: 092104
92 Yang J, Chen Y, Peng J, et al. Synthesis of $CoSb_3$ skutterudite by mechanical alloying. J Alloys Compd, 2004, 375: 229–232
93 Tan Q, Zhao L D, Li J F, et al. Thermoelectrics with earth abundant elements: Low thermal conductivity and high thermopower in doped SnS. J Mater Chem A, 2014, 2: 17302–17306
94 Wei T R, Wang H, Gibbs Z M, et al. Thermoelectric properties of Sn-doped p-type Cu_3SbSe_4: A compound with large effective mass and small band gap. J Mater Chem A, 2014, 2: 13527–13533
95 May A F, Fleurial J P, Snyder G J. Thermoelectric performance of lanthanum telluride produced via mechanical alloying. Phys Rev B, 2008, 78: 125205
96 Umemoto M. Preparation of thermoelectric β-$FeSi_2$ doped with Al and Mn by mechanical alloying (*overview*). Mater Trans JIM, 1995, 36: 373–383
97 Wei T R, Wu C F, Sun W, et al. Is Cu_3SbSe_3 a promising thermoelectric material? RSC Adv, 2015, 5: 42848–42854
98 Zou M, Li J F, Du B, et al. Fabrication and thermoelectric properties of fine-grained TiNiSn compounds. J Solid State Chem, 2009, 182: 3138–3142
99 Zou M, Li J F, Guo P, et al. Synthesis and thermoelectric properties of fine-grained FeVSb system half-Heusler compound polycrystals with high phase purity. J Phys D Appl Phys, 2010, 43: 415403
100 Kanatzia A, Papageorgiou C, Lioutas C, et al. Design of ball-milling experiments on Bi_2Te_3 thermoelectric material. J Elec Mater, 2013, 42: 1652–1660
101 Zhang Q, Wang H, Liu W, et al. Enhancement of thermoelectric figure-of-merit by resonant states of aluminium doping in lead selenide. Energ Environ Sci, 2012, 5: 5246–5251
102 Li Z Y, Li J F. Fine-grained and nanostructured $AgPb_mSbTe_{m+2}$ alloys with high thermoelectric figure of merit at medium temperature. Adv Energ Mater, 2014, 4: 1300937
103 Xing Z B, Li Z Y, Tan Q, et al. Composition optimization of p-type $AgSn_mSbTe_{m+2}$ thermoelectric materials synthesized by mechanical alloying and spark plasma sintering. J Alloys Compd, 2014, 615: 451–455
104 Liu W S, Zhang B P, Li J F, et al. Enhanced thermoelectric properties in $CoSb_{3-x}Te_x$ alloys prepared by mechanical alloying and spark plasma sintering. J Appl Phys, 2007, 102: 103717–103717
105 Liu W S, Zhang B P, Zhao L D, et al. Improvement of thermoelectric performance of $CoSb_{3-x}Te_x$ skutterudite compounds by additional substitution of IVB-group elements for Sb. Chem Mater, 2008, 20: 7526–7531
106 Tan Q, Li J F. Thermoelectric properties of Sn-S bulk materials prepared by mechanical alloying and spark plasma sintering. J Elec Mater, 2014, 43: 2435–2439
107 Pele V, Barreteau C, Berardan D, et al. Direct synthesis of BiCuChO-type oxychalcogenides by mechanical alloying. J Solid State Chem, 2013, 203: 187–191
108 Tang X, Xie W, Li H, et al. Preparation and thermoelectric transport properties of high-performance p-type Bi_2Te_3 with layered nanostructure. Appl Phys Lett, 2007, 90: 012102
109 Xie W, Tang X, Yan Y, et al. High thermoelectric performance BiSbTe alloy with unique low-dimensional structure. J Appl Phys, 2009, 105: 113713
110 Xie W, Wang S, Zhu S, et al. High performance Bi_2Te_3 nanocomposites prepared by single-element-melt-spinning spark-plasma sintering. J Mater Sci, 2013, 48: 2745–2760
111 Tkatch V I, Denisenko S N, Beloshov O N. Direct measurements of the cooling rates in the single roller rapid solidification technique. Acta Mater, 1997, 45: 2821–2826
112 Tan G, Liu W, Wang S, et al. Rapid preparation of $CeFe_4Sb_{12}$ skutterudite by melt spinning: Rich nanostructures and high thermoelectric performance. J Mater Chem A, 2013, 1: 12657–12668
113 Xie W, He J, Kang H J, et al. Identifying the specific nanostructures responsible for the high thermoelectric performance of $(Bi,Sb)_2Te_3$ Nanocomposites. Nano Lett, 2010, 10: 3283–3289
114 Tkatch V I, Limanovskii A I, Denisenko S N, et al. The effect of the melt-spinning processing parameters on the rate of cooling. Mater Sci Eng-A, 2002, 323: 91–96
115 Pond R B. Metallic Filaments and Method of Making Same. US Patent No. 2825108, 1958
116 Pond R B. Apparatus for Producing Alloy and Bimetallic Filaments. US Patent No. 2900708, 1959
117 Pond R B, Maddin R. Method of producing rapidly solidified filamentary castings. Trans Met Soc AIME, 1969, 245: 2475–2476
118 Dey T K. Electrical conductivity, thermoelectric power and figure of merit of doped Bi-Sb tapes produced by melt spinning technique. Pramana J Phys, 1990, 34: 243–248
119 Lee S M, Okamoto Y, Kawahara T, et al. The fabrication and thermoelectric properties of amorphous Si-Ge-Au bulk samples. MRS Proc, 2001, 691: G8-9
120 Kim T S, Kim I S, Kim T K, et al. Thermoelectric properties of p-type $25\%Bi_2Te_3+75\%Sb_2Te_3$ alloys manufactured by rapid solidification and hot pressing. Mater Sci Eng B, 2002, 90: 42–46
121 Chen H Y, Zhao X B, Lu Y F, et al. Microstructures and thermoelectric properties of $Fe_{0.92}Mn_{0.08}Six$ alloys prepared by rapid solidification and hot pressing. J Appl Phys, 2003, 94: 6621–6626
122 Zhao X B, Chen H Y, Müller E, et al. Microstructure development of Fe_2Si_5 thermoelectric alloys during rapid solidification, hot pressing and annealing. J Alloys Compd, 2004, 365: 206–210
123 Wang S, Xie W, Li H, et al. Enhanced performances of melt spun $Bi_2(Te,Se)_3$ for n-type thermoelectric legs. Intermetallics, 2011, 19: 1024–1031
124 Li H, Tang X, Su X, et al. Preparation and thermoelectric properties of high-performance Sb additional $Yb_{0.2}Co_4Sb_{12+y}$ bulk materials with nanostructure. Appl Phys Lett, 2008, 92: 202114
125 Thompson D R, Liu C, Yang J, et al. Rare-earth free p-type filled skutterudites: Mechanisms for low thermal conductivity and effects of Fe/Co ratio on the band structure and charge transport. Acta Mater, 2015, 92: 152–162
126 Luo W, Li H, Fu F, et al. Improved thermoelectric properties of Al-doped higher manganese silicide prepared by a rapid solidification method. J Elec Mater, 2011, 40: 1233–1237
127 Zhang Q, Zheng Y, Su X, et al. Enhanced power factor of $Mg_2Si_{0.3}Sn_{0.7}$ synthesized by a non-equilibrium rapid solidification method. Scripta Mater, 2015, 96: 1–4

128 Yu C, Zhu T J, Xiao K, et al. Reduced grain size and improved thermoelectric properties of melt spun (Hf,Zr)NiSn half-heusler alloys. J Elec Mater, 2010, 39: 2008–2012
129 Wang S, Li H, Qi D, et al. Enhancement of the thermoelectric performance of β-Zn_4Sb_3 by *in situ* nanostructures and minute Cd-doping. Acta Mater, 2011, 59: 4805–4817
130 Zhu T, Gao H, Chen Y, et al. Ioffe-regel limit and lattice thermal conductivity reduction of high performance $(AgSbTe_2)_{15}(GeTe)_{85}$ thermoelectric materials. J Mater Chem A, 2014, 2: 3251–3256
131 Sikalidis C. Advances in Ceramics-Synthesis and Characterization, Processing and Specific Applications. Croatia: InTech Publisher, 2011
132 Sytschev A E, Merzhanov A G. Self-propagating high-temperature synthesis of nanomaterials. Russ Chem Rev, 2004, 73: 147–159
133 Zheng G, Su X, Liang T, et al. High thermoelectric performance of mechanically robust n-type $Bi_2Te_{3-x}Se_x$ prepared by combustion synthesis. J Mater Chem A, 2015, 3: 6603–6613
134 Liang T, Su X, Tan X, et al. Ultra-fast non-equilibrium synthesis and phase segregation in In_xSn_{1-x} Te thermoelectrics by SHS-PAS processing. J Mater Chem C, 2015, 3: 8550–8558
135 Delgado A, Cordova S, Lopez I, et al. Mechanically activated combustion synthesis and shockwave consolidation of magnesium silicide. J Alloys Compd, 2016, 658: 422–429
136 Zhang Q, Su X, Yan Y, et al. Phase segregation and superior thermoelectric properties of $Mg_2Si_{1-x}Sb_x$ ($0 \leqslant x \leqslant 0.025$) prepared by ultrafast self-propagating high-temperature synthesis. ACS Appl Mater Interface, 2016, 8: 3268–3276
137 Liang T, Su X, Yan Y, et al. Ultra-fast synthesis and thermoelectric properties of Te doped skutterudites. J Mater Chem A, 2014, 2: 17914–17918
138 Ren G K, Lan J, Butt S, et al. Enhanced thermoelectric properties in Pb-doped BiCuSeO oxyselenides prepared by ultrafast synthesis. RSC Adv, 2015, 5: 69878–69885
139 Selig J, Lin S, Lin H T, et al. Economical route to produce high Seebeck coefficient calcium cobaltate for bulk thermoelectric applications. J Am Ceram Soc, 2011, 94: 3245–3248
140 Lin S, Selig J. Self-propagating high-temperature synthesis of $Ca_{1.24}Co_{1.62}O_{3.86}$ thermoelectric powders. J Alloys Compd, 2010, 503: 402–409
141 Li Y, Liu G, Cao T, et al. Enhanced thermoelectric properties of Cu_2SnSe_3 by (Ag,In)-Co-doping. Adv Funct Mater, 2016, 26: 6025–6032
142 Bux S K, Fleurial J P, Kaner R B. Nanostructured materials for thermoelectric applications. Chem Commun, 2010, 46: 8311–8324
143 Fitriani , Ovik R, Long B D, et al. A review on nanostructures of high-temperature thermoelectric materials for waste heat recovery. Renew Sustain Energ Rev, 2016, 64: 635–659
144 Shi W, Song S, Zhang H. Hydrothermal synthetic strategies of inorganic semiconducting nanostructures. Chem Soc Rev, 2013, 42: 5714–5743
145 Gharleghi A, Chu Y H, Lin F H, et al. Optimization and analysis of thermoelectric properties of unfilled $Co_{1-x-y}Ni_xFe_ySb_3$ synthesized via a rapid hydrothermal procedure. ACS Appl Mater Interface, 2016, 8: 5205–5215
146 Ju H, Kim J. Chemically exfoliated SnSe nanosheets and their SnSe/poly (3,4-ethylenedioxythiophene): Poly (styrenesulfonate) composite films for polymer based thermoelectric applications. ACS Nano, 2016, 10: 5730–5739
147 Cao Y Q, Zhao X B, Zhu T J, et al. Syntheses and thermoelectric properties of Bi_2Te_3/Sb_2Te_3 bulk nanocomposites with laminated nanostructure. Appl Phys Lett, 2008, 92: 143106
148 Zhang H T, Luo X G, Wang C H, et al. Characterization of nanocrystalline bismuth telluride (Bi_2Te_3) synthesized by a hydrothermal method. J Cryst Growth, 2004, 265: 558–562
149 Zhao X B, Ji X H, Zhang Y H, et al. Hydrothermal synthesis and microstructure investigation of nanostructured bismuth telluride powder. Appl Phys A, 2005, 80: 1567–1571
150 Fu J, Song S, Zhang X, et al. Bi_2Te_3 nanoplates and nanoflowers: Synthesized by hydrothermal process and their enhanced thermoelectric properties. Cryst Eng Comm, 2012, 14: 2159–2165
151 Liu C J, Lai H C, Liu Y L, et al. High thermoelectric figure-of-merit in p-type nanostructured $(Bi,Sb)_2Te_3$ fabricated via hydrothermal synthesis and evacuated-and-encapsulated sintering. J Mater Chem, 2012, 22: 4825–4831
152 Mi J L, Lock N, Sun T, et al. Biomolecule-assisted hydrothermal synthesis and self-assembly of Bi_2Te_3 nanostring-cluster hierarchical structure. ACS Nano, 2010, 4: 2523–2530
153 Zhao X B, Ji X H, Zhang Y H, et al. Bismuth telluride nanotubes and the effects on the thermoelectric properties of nanotube-containing nanocomposites. Appl Phys Lett, 2005, 86: 062111
154 Ji X, Zhang B, Tritt T M, et al. Solution-chemical syntheses of nanostructured Bi_2Te_3 and PbTe thermoelectric materials. J Elec Mater, 2007, 36: 721–726
155 Yokoyama S, Sato K, Muramatsu M, et al. Green synthesis and formation mechanism of nanostructured Bi_2Te_3 using ascorbic acid in aqueous solution. Adv Powder Tech, 2015, 26: 789–796
156 Wang Q, Fang Y, Yin H, et al. Inhomogenous doping induced the imperfect self-assembly of nanocrystals for the synthesis of porous $AgPb_{10}BiTe_{12}$ nanosheets and their thermoelectric transport properties. Chem Commun, 2015, 51: 1594–1596
157 Li Y, Li F, Dong J, et al. Enhanced mid-temperature thermoelectric performance of textured SnSe polycrystals made of solvothermally synthesized powders. J Mater Chem C, 2016, 4: 2047–2055
158 Yu S, Yang J, Wu Y, et al. A new low temperature one-step route to metal chalcogenide semiconductors: PbE, Bi_2E_3 (E = S, Se, Te). J Mater Chem, 1998, 8: 1949–1951
159 Deng Y, Wei G D, Nan C W. Ligand-assisted control growth of chain-like nanocrystals. Chem Phys Lett, 2003, 368: 639–643
160 Hong M, Chasapis T C, Chen Z G, et al. *n*-Type $Bi_2Te_{3-x}Se_x$ nanoplates with enhanced thermoelectric efficiency driven by wide-frequency phonon scatterings and synergistic carrier scatterings. ACS Nano, 2016, 10: 4719–4727
161 Ibáñez M, Luo Z, Genç A, et al. High-performance thermoelectric nanocomposites from nanocrystal building blocks. Nat Commun, 2016, 7: 10766
162 Mehta R J, Zhang Y, Karthik C, et al. A new class of doped nanobulk high-figure-of-merit thermoelectrics by scalable bottom-up assembly. Nat Mater, 2012, 11: 233–240
163 Baghbanzadeh M, Carbone L, Cozzoli P D, et al. Microwave-assisted synthesis of colloidal inorganic nanocrystals. Angew Chem Int Ed, 2011, 50: 11312–11359
164 Tsuji M, Hashimoto M, Nishizawa Y, et al. Microwave-assisted synthesis of metallic nanostructures in solution. Chem-Eur J, 2005, 11: 440–452
165 Li Z, Chen Y, Li J F, et al. Systhesizing SnTe nanocrystals leading to thermoelectric performance enhancement via an ultra-fast microwave hydrothermal method. Nano Energ, 2016, 28: 78–86
166 Nüchter M, Ondruschka B, Bonrath W, et al. Microwave assisted synthesis—A critical technology overview. Green Chem, 2004, 6: 128–141
167 Jin R, Liu J, Li G. Facile solvothermal synthesis, growth mechanism and thermoelectric property of flower-like Bi_2Te_3. Cryst Res Tech, 2014, 49: 460–466
168 Ciriminna R, Fidalgo A, Pandarus V, et al. The sol-gel route to advanced silica-based materials and recent applications. Chem Rev, 2013, 113: 6592–6620
169 Fan F J, Yu B, Wang Y X, et al. Colloidal synthesis of $Cu_2CdSnSe_4$ nanocrystals and hot-pressing to enhance the thermoelectric figure-of-merit. J Am Chem Soc, 2011, 133: 15910–15913
170 Butt S, Xu W, He W Q, et al. Enhancement of thermoelectric performance in Cd-doped $Ca_3Co_4O_9$ via spin entropy, defect chemistry and phonon scattering. J Mater Chem A, 2014, 2: 19479–19487

171 Li F, Li J F. Enhanced thermoelectric performance of separately Ni-doped and Ni/Sr-codoped $LaCoO_3$ nanocomposites. J Am Chem Soc, 2012, 95: 3562–3568
172 Ji X H, Zhao X B, Zhang Y H, et al. Solvothermal synthesis and thermoelectric properties of lanthanum contained Bi–Te and Bi–Se–Te alloys. Mater Lett, 2005, 59: 682–685
173 Hong M, Chen Z G, Yang L, et al. Enhancing thermoelectric performance of Bi_2Te_3-based nanostructures through rational structure design. Nanoscale, 2016, 8: 8681–8686
174 Dong G H, Zhu Y J, Chen L D. Microwave-assisted rapid synthesis of Sb_2Te_3 nanosheets and thermoelectric properties of bulk samples prepared by spark plasma sintering. J Mater Chem, 2010, 20: 1976–1981
175 Zhou W, Zhao W, Lu Z, et al. Preparation and thermoelectric properties of sulfur doped Ag_2Te nanoparticles via solvothermal methods. Nanoscale, 2012, 4: 3926–3931
176 Yang H Q, Miao L, Liu C Y, et al. Solvothermal synthesis of wire-like $Sn_xSb_2Te_{3+x}$ with an enhanced thermoelectric performance. Dalton Trans, 2016, 45: 7483–7491
177 Tan Q, Wu C F, Sun W, et al. Solvothermally synthesized SnS nanorods with high carrier mobility leading to thermoelectric enhancement. RSC Adv, 2016, 6: 43985–43988
178 James D J, Lu X, Morelli D T, et al. Solvothermal synthesis of tetrahedrite: Speeding up the process of thermoelectric material generation. ACS Appl Mater Interface, 2015, 7: 23623–23632
179 Zhu Y, Shen H, Guan H. Microwave-assisted synthesis and thermoelectric properties of $CoSb_3$ compounds. J Mater Sci-Mater Electron, 2012, 23: 2210–2215
180 Bloxam A. Improved manufacture of electric incandescence lamp laments from tungsten or molybdenum or an alloy thereof. GB Patent, 1906, 27: 13
181 Inoue K. Electric-Discharge Sintering. US Patent No. 3241956, 1966
182 Zhang Q, Ai X, Wang L, et al. Improved thermoelectric performance of silver nanoparticles-dispersed Bi_2Te_3 composites deriving from hierarchical two-phased heterostructure. Adv Funct Mater, 2015, 25: 966–976
183 Soni A, Shen Y, Yin M, et al. Interface driven energy filtering of thermoelectric power in spark plasma sintered $Bi_2Te_{2.7}Se_{0.3}$ nanoplatelet composites. Nano Lett, 2012, 12: 4305–4310
184 Aminorroaya Yamini S, Brewis M, Byrnes J, et al. Fabrication of thermoelectric materials—Thermal stability and repeatability of achieved efficiencies. J Mater Chem C, 2015, 3: 10610–10615
185 He Y, Lu P, Shi X, et al. Ultrahigh thermoelectric performance in mosaic crystals. Adv Mater, 2015, 27: 3639–3644
186 Liu Y, Lin Y, Shi Z, et al. Preparation of $Ca_3Co_4O_9$ and improvement of its thermoelectric properties by spark plasma sintering. J Am Ceram Soc, 2005, 88: 1337–1340
187 Li X Y, Chen L D, Fan J F, et al. Thermoelectric properties of Te-doped $CoSb_3$ by spark plasma sintering. J Appl Phys, 2005, 98: 083702
188 Souma T, Nakamoto G, Kurisu M. Low-temperature thermoelectric properties of α- and β-Zn_4Sb_3 bulk crystals prepared by a gradient freeze method and a spark plasma sintering method. J Alloys Compd, 2002, 340: 275–280
189 Kim K H, Shim S H, Shim K B, et al. Microstructural and thermoelectric characteristics of zinc oxide-based thermoelectric materials fabricated using a spark plasma sintering process. J Am Ceram Soc, 2005, 88: 628–632
190 Kuo C H, Hwang C S, Jeng M S, et al. Thermoelectric transport properties of bismuth telluride bulk materials fabricated by ball milling and spark plasma sintering. J Alloys Compd, 2010, 496: 687–690
191 Munir Z A, Anselmi-Tamburini U, Ohyanagi M. The effect of electric field and pressure on the synthesis and consolidation of materials: A review of the spark plasma sintering method. J Mater Sci, 2006, 41: 763–777
192 Omori M. Sintering, consolidation, reaction and crystal growth by the spark plasma system (SPS). Mater Sci Eng A, 2000, 287: 183–188
193 Guillon O, Gonzalez-Julian J, Dargatz B, et al. Field-assisted sintering technology/spark plasma sintering: Mechanisms, materials, and technology developments. Adv Eng Mater, 2014, 16: 830–849
194 Liu H, Shi X, Xu F, et al. Copper ion liquid-like thermoelectrics. Nat Mater, 2012, 11: 422–425
195 Meng Q L, Kong S, Huang Z, et al. Simultaneous enhancement in the power factor and thermoelectric performance of copper sulfide by In_2S_3 doping. J Mater Chem A, 2016, 4: 12624–12629
196 Qiu W, Xi L, Wei P, et al. Part-crystalline part-liquid state and rattling-like thermal damping in materials with chemical-bond hierarchy. Proc Natl Acad Sci USA, 2014, 111: 15031–15035
197 Kirkham M, Majsztrik P, Skoug E, et al. High-temperature order/disorder transition in the thermoelectric Cu_3SbSe_3. J Mater Res, 2011, 26: 2001–2005
198 Toberer E S, Cox C A, Brown S R, et al. Traversing the metal-insulator transition in a zintl phase: Rational enhancement of thermoelectric efficiency in $Yb_{14}Mn_{1-x}Al_xSb_{11}$. Adv Funct Mater, 2008, 18: 2795–2800
199 Tyagi K, Gahtori B, Bathula S, et al. Thermoelectric properties of Cu_3SbSe_3 with intrinsically ultralow lattice thermal conductivity. J Mater Chem A, 2014, 2: 15829–15835
200 Yan X, Poudel B, Ma Y, et al. Experimental studies on anisotropic thermoelectric properties and structures of n-type $Bi_2Te_{2.7}Se_{0.3}$. Nano Lett, 2010, 10: 3373–3378
201 Sui J, Li J, He J, et al. Texturation boosts the thermoelectric performance of BiCuSeO oxyselenides. Energ Environ Sci, 2013, 6: 2916–2920
202 Jiang Q, Yan H, Khaliq J, et al. Large *ZT* enhancement in hot forged nanostructured p-type $Bi_{0.5}Sb_{1.5}Te_3$ bulk alloys. J Mater Chem A, 2014, 2: 5785–5790
203 Shen J J, Zhu T J, Zhao X B, et al. Recrystallization induced *in situ* nanostructures in bulk bismuth antimony tellurides: A simple top down route and improved thermoelectric properties. Energ Environ Sci, 2010, 3: 1519–1523
204 Medlin D L, Snyder G J. Interfaces in bulk thermoelectric materials. Curr Opin Colloid In, 2009, 14: 226–235
205 Mikami M, Guilmeau E, Funahashi R, et al. Enhancement of electrical properties of the thermoelectric compound $Ca_3Co_4O_9$ through use of large-grained powder. J Mater Res, 2005, 20: 2491–2497
206 Ur S C, Nash P, Kim I H. Thermoelectric properties of Zn_4Sb_3 processed by sinter-forging. Mater Lett, 2004, 58: 2937–2941
207 Yamashita O, Tomiyoshi S. Effect of Annealing on thermoelectric properties of bismuth telluride compounds. Jpn J Appl Phys, 2003, 42: 492–500
208 Schultz J M, McHugh J P, Tiller W A. Effects of heavy deformation and annealing on the electrical properties of Bi_2Te_3. J Appl Phys, 1962, 33: 2443–2450
209 Zhao L D, Zhang B P, Liu W S, et al. Effects of annealing on electrical properties of n-type Bi_2Te_3 fabricated by mechanical alloying and spark plasma sintering. J Alloys Compd, 2009, 467: 91–97
210 Schumacher C, Reinsberg K G, Rostek R, et al. Optimizations of pulsed plated p- and n-type Bi_2Te_3-based ternary compounds by annealing in different ambient atmospheres. Adv Energ Mater, 2013, 3: 95–104
211 Zhou M, Li J F, Kita T. Nanostructured $AgPb_mSbTe_{m+2}$ system bulk materials with enhanced thermoelectric performance. J Am Chem Soc, 2008, 130: 4527–4532